

# **Metal-Organic Framework-Based Drug Delivery for Treatment of Tuberculosis**

**M.Sc. Thesis**

By  
**Dhwani Thakkar**



**DEPARTMENT OF BIOSCIENCES AND BIOMEDICAL  
ENGINEERING  
INDIAN INSTITUTE OF TECHNOLOGY INDORE  
MAY 2024**



# **Metal-Organic Framework-Based Drug Delivery for Treatment of Tuberculosis**

**A THESIS**

*Submitted in partial fulfillment of the  
requirements for the award of the degree  
of*  
**Master of Science**

*by*  
**Dhwani Thakkar**



**DEPARTMENT OF BIOSCIENCES AND BIOMEDICAL  
ENGINEERING  
INDIAN INSTITUTE OF TECHNOLOGY INDORE  
MAY 2024**





# INDIAN INSTITUTE OF TECHNOLOGY INDORE

## CANDIDATE'S DECLARATION

I hereby certify that the work which is being presented in the thesis entitled **Metal-Organic Framework-Based Drug Delivery for Treatment of Tuberculosis** in the partial fulfillment of the requirements for the award of the degree of **MASTER OF SCIENCE** and submitted in the **DEPARTMENT OF BIOSCIENCES AND BIOMEDICAL ENGINEERING, Indian Institute of Technology Indore**, is an authentic record of my own work carried out during the time period from July 2022 to May 2024 under the supervision of **Prof. Avinash Sonawane**, Professor, Department of Biosciences and Biomedical Engineering.

The matter presented in this thesis has not been submitted by me for the award of any other degree of this or any other institute.

*Dhwani*  
24.05.24

Signature of the student with date  
**Dhwani Thakkar**

-----  
This is to certify that the above statement made by the candidate is correct to the best of my/our knowledge.

*Avinash*  
24.05.2024

Signature of the supervisor of M.Sc. with date  
**Prof. Avinash Sonawane**

-----  
Dhwani Thakkar has successfully given her M.Sc. Oral Examination held on  
**10 May 2024**

*Avinash*  
Signature(s) of Supervisor(s) of MSc thesis  
Date: 24.05.2024

Convener, DPGC  
Date:



## ACKNOWLEDGEMENTS

I take this opportunity to express my heartfelt gratitude to all those who have played a role in my academic journey. Completing this M.Sc. thesis would not have been possible without the support, guidance, and encouragement of my supervisor, **Prof. Avinash Sonawane**. His invaluable guidance and support throughout this project, his expertise, insightful comments, and constructive feedback have been instrumental in shaping my research and in guiding me towards the right direction. I am grateful to him for his unwavering belief in my abilities and for his continuous encouragement throughout this journey.

I sincerely thank our HoD, Prof. Amit Kumar, our course coordinator Dr. Parimal Kar and DPGC Prof. Prashant Kodgire. I would also like to express my sincere thanks to the faculty members of the Department of Biosciences and Biomedical Engineering, Indian Institute of Technology, Indore, for their support and encouragement during my academic journey. The stimulating academic environment and the challenging coursework have been instrumental in developing my critical thinking and research skills. I am grateful to my professors for their inspiring lectures, insightful comments, and valuable feedback that have helped me grow as a researcher and as an individual.

Moreover, I would like to extend my sincere appreciation to my Lab mates who generously shared their time and knowledge, without whom this research would not have been possible. Their willingness to participate and to share their personal experiences and perspectives have been invaluable in shaping the research findings. I am grateful to Ms. Suchi Chaturvedi, Ms. Barsa Nayak, Mr. Sibi Karthik and Mr. Kishan Khandelwal for helping me at each difficult moment. I would also like to thank Ms. Bhagyashree Nayak, Ms. Sukanya Samata and Ms. Bidisha Choudhury for supporting me.

I am grateful to my friends, Mr. Shivmuni Sarup, Ms. Ritika Sharma, and Mr. Kanav Gupta, for their constant support and encouragement.

I would like to express my deepest gratitude to my parents, Mr. Atul Thakkar and Mrs. Jayana Thakkar, for their unwavering support, encouragement, and love throughout my academic journey. Their sacrifices, guidance, and belief in my abilities have been the cornerstone of my success. Their endless encouragement and understanding have provided me with the strength and motivation to overcome challenges and pursue my aspirations.

**Dedicated to my parents**



## ABSTRACT

Tuberculosis (TB) is globally recognized as the second most fatal disease after HIV and AIDS. Due to the multi-drug resistant (MDR) and extensively drug-resistant (XDR) properties of *M. tuberculosis*, it is becoming difficult to treat the patients. Major drawbacks of already available antibiotics for TB treatment are high dose administration, poor bioavailability, and low biodegradability. To overcome this problem, we tried to develop a novel drug delivery system that would deliver the drug specifically to the infected macrophages. In this work, we have encapsulated the well-known first-line anti-TB drug Rifampin (RIF) into the Zeolitic Imidazole Framework (ZIF-8). Successful encapsulation of Rifampin into ZIF-8 was confirmed by different characterization techniques such as UV-Vis spectroscopy, FT-IR, TGA, TEM, SEM, BET analysis and PXRD. Further pH-responsive drug release and fluorescence studies and reduced cell cytotoxicity confirm that RIF-loaded ZIF-8 can be treated as a suitable candidate for the delivery of anti-tubercular agents and reveal the potential application for tuberculosis treatment. Overall, this thesis contributes to the burgeoning field of MOF-based drug delivery systems, offering valuable insights into their application for TB treatment. The findings underscore the promising potential of ZIF-8 as a versatile platform for the controlled delivery of anti-TB drugs, paving the way for future advancements in targeted therapeutic interventions against tuberculosis.

Keywords: Metal-organic framework, tuberculosis, rifampicin, ZIF-8, drug delivery, cytotoxicity, cellular uptake, pH-responsive release.



## **PUBLICATION**

1. Dhwani Thakkar, Anulipsa Priyadarsini, Rojalin Sahu, Avinash Sonawane\*. Development of pH-responsive drug delivery system for delivery of rifampicin for treatment of tuberculosis. (Manuscript under preparation)



# TABLE OF CONTENTS

## List of figures

## List of abbreviations

<b>Chapter 1: Introduction...</b>	<b>1</b>
1.1 Global scenario of tuberculosis...	1
1.2 Overview of <i>Mycobacterium tuberculosis</i> infection...	2
1.3 Current treatment for tuberculosis...	4
1.4 Mechanism of action of first and second line of drugs...	5
1.5 Drawbacks of current tuberculosis treatment...	7
1.6 Nanocarrier-based drug delivery in tuberculosis...	8
1.7 Metal-organic frameworks...	10
1.8 Applications of metal-organic frameworks in drug delivery...	13
1.9 Organisation of thesis...	15
<b>Chapter 2: Literature Review</b>	<b>17</b>
2.1 Overview...	17
2.2 Antibacterial mechanisms of MOF-based nanomedicines...	17
<b>Chapter 3: Objectives of the thesis</b>	<b>21</b>
<b>Chapter 4: Materials and Methods</b>	<b>23</b>
4.1 Materials...	23
4.2 Synthesis of zeolitic imidazolate framework-8 (ZIF-8)...	23
4.3 Activation of ZIF-8...	24
4.4 Rifampicin encapsulation within the ZIF-8 framework...	24
4.5 Characterization of rifampicin encapsulated ZIF-8...	25
4.6 Cell line and cell culture conditions...	28
4.7 <i>In-vitro</i> drug release assay...	28

4.8 Cell viability studies.....	29
4.9 Cellular uptake assay.....	30

**Chapter 5: Results and Discussion ..... 31**

5.1 Characterization of synthesized ZIF-8 via powdered X-ray diffraction (PXRD) .....	31
5.2 Characterization of synthesized ZIF-8 via Fourier-Transform Infrared Spectroscopy (FTIR).....	32
5.3 Activation of ZIF-8 .....	33
5.4 Encapsulation of rifampicin in ZIF-8 (RIF@ZIF-8) .....	34
5.5 Confirmation of encapsulation using UV-Vis spectroscopy.....	36
5.6 Morphology and surface analysis using scanning electron microscopy (SEM) and energy dispersive X-rays spectroscopy (EDS).....	37
5.7 Thermal stability analysis of ZIF-8 and RIF@ZIF-8.....	38
5.8 Surface area analysis of ZIF-8 and RIF@ZIF-8.....	39
5.9 In-vitro pH-responsive release of rifampicin.....	40
5.10 In-vitro cytotoxicity study.....	42
5.11 Cellular uptake of RIF@ZIF-8.....	43

**Chapter 6: Conclusion and Future Directions ..... 45**

**References... ..... 47**

## LIST OF FIGURES

1.1 Estimated TB incidence rates in 2022...	1
1.2 Pathogenesis of Tuberculosis...	3
1.3 Available drugs for TB...	5
1.4 Schematic diagram representing the desired profile for developing new tuberculosis drugs...	8
1.5 Various nanoparticles explored for treatment of tuberculosis...	10
1.6 Formation of MOF structure...	11
1.7 Methods of MOF synthesis...	12
1.8 Properties of MOF...	12
1.9 MOF-based stimuli-responsive system for drug delivery...	14
2.1 MOF-based treatment of intracellular infection...	18
4.1 Chemical reaction of MTT assay...	29
5.1 PXRD spectra of synthesized ZIF-8...	31
5.2 FTIR spectra of ZIF-8...	33
5.3 PXRD spectra of ZIF-8 after activation...	34
5.4 Absorption spectra of rifampicin...	35
5.5 Calibration curve of rifampicin...	35
5.6 UV-Visible spectra of RIF, ZIF-8 and RIF@ZIF-8...	36
5.7 SEM and EDS analysis of ZIF-8...	37
5.8 SEM and EDS analysis of RIF@ZIF-8...	38
5.9 TGA Analysis of ZIF-8 (black line) and RIF@ZIF-8 (red line)...	39

5.10 Nitrogen Adsorption isotherm of ZIF-8 (A) and RIF@ZIF-8 (B).....	40
5.11 Drug release profile of rifampicin from RIF@ZIF-8 at three different pH.....	41
5.12 Cell viability of ZIF-8, RIF@ZIF-8 and rifampicin at a concentration range of 0 to 100 µg/ml.....	42
5.13 Cellular uptake of RIF@ZIF-8 by RAW 264.7 macrophages.....	43

## LIST OF ABBREVIATIONS

TB.....	Tuberculosis
Mtb .....	<i>Mycobacterium tuberculosis</i>
MSmeg... ..	<i>Mycobacterium smegmatis</i>
MOFs.....	Metallic Organic Framework
E-MOF.....	Encapsulated MOFs
RIF@ZIF-8.....	Encapsulated MOFs
RIF.....	Rifampicin
INH.....	Isoniazid
PZA .....	Pyrazinamide
EMB... ..	Ethambutol
HIV.....	Human Immunodeficiency Virus
ZIF-8.....	Zeolitic Imidazolate Framework
TNF $\alpha$ .....	Tumor necrosis factor-alpha
NK .....	Natural killer cell
BCG.....	Bacillus Calmette-Guerin
CTLs.....	Cytotoxic T lymphocytes
INF $\gamma$ .....	Interferon
IL... ..	Interleukin
ER.....	Endoplasmic reticulum
DOT.....	Directly Observed Treatment

MHC.....Major histocompatibility complex  
MDR TB .....Multidrug resistant TB  
XDR TB... ..Extensively drug-resistant TB  
TDR TB.....Totally drug-resistant TB  
RR TB... ..Rifampicin resistant TB  
FQ.....Fluoroquinolones  
MIC... ..Minimum Inhibitory Concentration  
SM..... Streptomycin  
KM... ..Kanamycin  
AMK .....Amikacin  
LFX.....Levofloxacin  
MFX... ..Moxifloxacin  
CIP.....Ciprofloxacin  
AB... ..Antibiotic  
NP.....Nanoparticle

# Chapter 1

## Introduction

---

### 1.1 Global scenario of tuberculosis

*Mycobacterium tuberculosis* (*M. tuberculosis*) is an obligate, intracellular pathogenic agent that causes tuberculosis. Tuberculosis (TB) has been affecting humans for more than 70,000<sup>1</sup>. *Mycobacterium tuberculosis* was identified by Dr. Robert Koch a century ago<sup>2</sup>. However, still today, this pathogen remains a global threat to human health by being one of the major causes of morbidity and mortality. Over the course of human history, it has killed more people than any other pathogen, making it the deadliest infectious agent in the world until the emergence of SARS-COV-2 in 2019. In 2022, approximately 10.6 million people fell ill with TB, and 1.3 million died worldwide. 87% of world TB cases were shared by 30 countries, of which India accounted for the highest number of TB cases (28.2 lakhs), i.e., 27% of the global TB burden and an estimated 3.42 lakhs deaths, according to the global TB report released by the World Health Organization<sup>3</sup>.

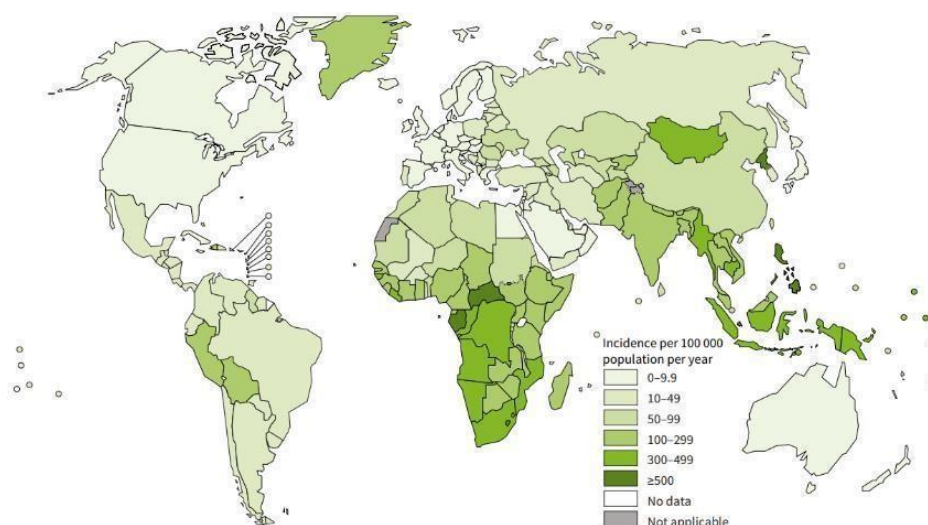


**Figure 1.1:** Estimated TB incidence rates in 2022<sup>3</sup>.

## **1.2 Overview of *Mycobacterium tuberculosis* infection**

*M. tuberculosis* mainly infects lungs causing pulmonary TB, however, it can also cause disease in other tissues and organs such as brain, lymph nodes, kidneys and spine leading to extrapulmonary TB. The pathogenic agent of tuberculosis is transmitted via inhalation of aerosol droplets (dried mucous droplets) containing bacteria expelled by a person having active tuberculosis disease. The number of *M. tuberculosis* required to establish infection is very low, estimated to be approximately three bacilli<sup>1,3</sup>. This shows the effectiveness of *M. tuberculosis* at evading immune responses.

The pathogen enters the host via the respiratory tract and moves through upper and lower airways where it can infect epithelial cells and microfold cells. Once it reaches lower respiratory tract, it interacts with tissue resident macrophages – alveolar macrophages present within alveolus and dendritic cells present within the interstitial space. Alveolar macrophages internalize *Mycobacterium* via receptor mediator phagocytosis with various different receptors recognizing specific pathogen associated molecular patterns. Macrophages have various strategies to eliminate bacteria such as production of antimicrobial peptides, generation of reactive oxygen and nitrogen species, acidification of phagosome and its fusion with lysosome, restricting important nutrients such as iron. However, *M. tuberculosis* has developed a variety of mechanisms to persist in macrophages. Only in a few individuals, the macrophages and, thus the innate immune responses are able to eliminate the bacteria completely<sup>4</sup>.

In most cases, macrophages are unsuccessful in getting rid of the bacteria; *M. tuberculosis* then moves on to infiltrate the interstitial tissue of the lung. This can happen when the mycobacteria infects the alveolar epithelium and transmigrates to the interstitium or when infected macrophages move into interstitial space. Subsequently, *M. tuberculosis* is delivered to the pulmonary lymph nodes by either dendritic cells or inflammatory monocytes to prime and activate B- and T- lymphocytes. This leads to the migration of numerous immune cells such as T lymphocytes, B cells,

neutrophils and macrophages into lung interstitium. The bacilli diversify their niche by infecting neutrophils, dendritic cells and recruited macrophages. This influx of immune cells at the site of infection leads to the formation of a characteristic structure known as granuloma, which is the histopathological hallmark of tuberculosis. Granulomas are organised aggregate of immune cells wherein the central core consists of macrophages, neutrophils, dendritic cells and fibroblasts. T and B lymphocytes are present in the periphery. As the immune cell accumulation progresses, cells in the centre faces hypoxic environment and undergoes necrotic cell death forming acellular core termed caseum<sup>3,4,5</sup>. From the perspective of the host, granulomas restrict the progression of infection and minimize tissue damage whereas from the perspective of mycobacteria, granuloma allows it to infect and replicate with a wide variety of immune cells and thus avoid clearance from the host.

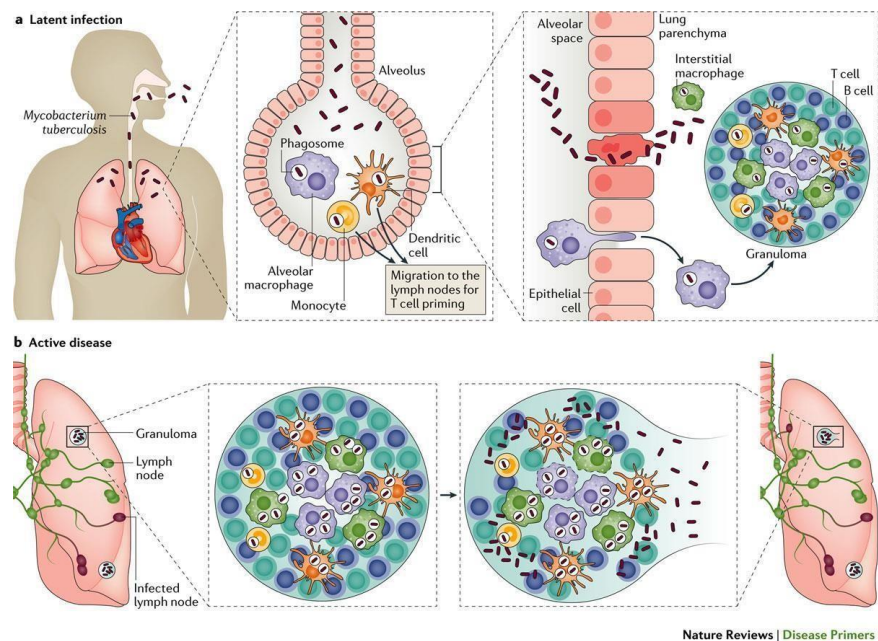


**Figure 1.2:** Pathogenesis of Tuberculosis<sup>3</sup>.

In most cases, the granuloma is able to contain the infection without inducing tissue damage. Such a condition is known as latent tuberculosis infection. However, in some individuals the granulomas are not able to withstand the bacterial load, leading to active tuberculosis disease<sup>5</sup>.

5-10% of the population with latent TB infection develop active disease later on, in some individuals even decades later. The risk of developing active TB disease increases in individuals suffering from AIDS, cancer, diabetes, kidney failure. Structure of granuloma changes during reactivation of disease. The central core of the caseum liquifies and creates a more favourable environment. *M. tuberculosis* can also disseminate to other organs via lymph nodes and the bloodstream<sup>2</sup>.

### **1.3 Current treatment for tuberculosis**

Chemotherapy is currently the only option for management of Tuberculosis worldwide. The cure rate is 95 % only if the treatment provided is correct and at the right time. Drug susceptible tuberculosis is treated with the following medication regimen. This therapeutic protocol involves either daily administration for a duration of two months or thrice-weekly administration for the same period, succeeded by a four-month course comprising isoniazid and rifampicin, alongside ethambutol (E), isoniazid (H), pyrazinamide (Z), rifampicin (R)<sup>6,7</sup>.

The complexity of treatment regimens has escalated due to the surge in tuberculosis (TB) complications, including multidrug-resistant (MDR) strains, extensively drug-resistant (XDR) strains, concurrent HIV infection, the presence of comorbidities such as diabetes, and the necessity for TB retreatment post-recurrence<sup>8</sup>. Managing drug-resistant TB may entail extending the treatment duration with drugs to which the organism remains susceptible for up to 20 months or incorporating an injectable antibiotic such as kanamycin, amikacin, or streptomycin to the regimen<sup>8,9</sup>.

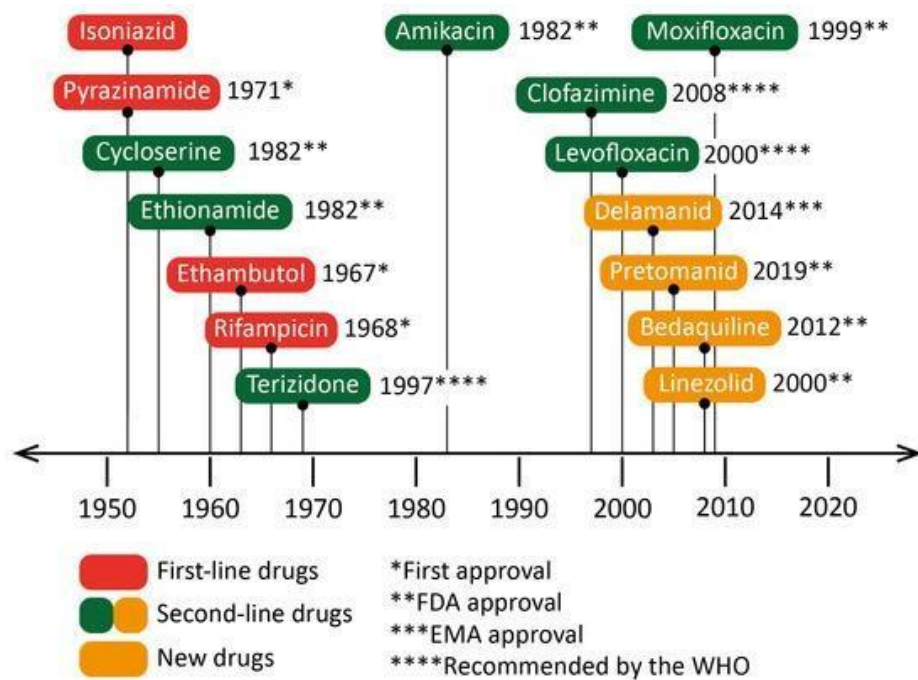


**Figure 1.3:** Available drugs for TB<sup>9</sup>.

## 1.4 Mechanism of action of first and second line of drugs

I. Rifampicin (RIF): The FDA approved this drug in 1971 and showed bactericidal activity. It inhibits the activity of DNA-dependent RNA polymerase of the MTB. It prevents RNA transcription and translation to proteins. Rifampicin-resistant (RR) strains cause mutation in the *rpoB* gene (encodes beta-subunit of DNA dependent RNA polymerase), which leads to protein synthesis and bacterial survival<sup>10</sup>.

II. Isoniazid (INH): Although the INH structure is more straightforward, the mechanism of action against MTB is quite complex. INH mainly targets the mycolic acid synthesis pathway. Activation of pro-drug INH takes place with the help of catalase-peroxidase (KatG). Further, activated form tightly binds with the ACP reductase *InhA*, an enzyme responsible for fatty acid elongation in MTB, and eventually restricts fatty acid synthesis. Isoniazid-resistant strains cause mutation in *KatG* as well as in the *InhA* gene frequently. Mutation in the *KatG* gene cannot activate pro-drug isoniazid in the same way mutation in the *InhA* gene cannot bind with Isoniazid drugs that can't resist mycolic acid synthesis<sup>11</sup>.

III. Pyrazinamide (PZA): First-line unique sterilizing drug that shows activity against semi-dormant bacteria with low metabolic activity. Synergistic action of PZA with RIF showed promising results in newly developed TB patients. It can only work in an acidic environment, making it different from other drugs<sup>12</sup>. PZA inhibits mycolic acid synthesis of non-growing bacilli. PZA (Pro-drug) is activated by an enzyme pyrazinamidase (PZase) into active pyrazinoic acid (POA). This active form inhibits the synthesis of FAS-I and FAS-II, which plays a role in fatty acid synthesis<sup>13</sup>.

IV. Ethambutol (EMB): This drug is more effective when used as combinational therapy. It is one of the bacteriostatic drugs. EMB inhibits the transfer of mycolic acid to the cell wall of MTB and restricts the biosynthesis of arabinogalactan<sup>14</sup>.

These four first-line drugs are mainly used as a combinational therapy that lasts for 6-7 months. Generally, EMB in synergy with INH is given in TB treatment. PZA with RIF and second-line drugs are also used in MDR cases with a more extended treatment duration<sup>15</sup>.

### **Second-line drugs and mode of action:**

I. Fluoroquinolones (FQ): Ciprofloxacin, levofloxacin, cycloserine, clofazimine, moxifloxacin, gatifloxacin etc. These drugs work by inhibiting topoisomerase 2 (DNA gyrase) and thereby stops the replication fork movement and transcription<sup>16</sup>.

II. Injectable: Kanamycin, capreomycin, amikacin, viomycin. These drugs work by inhibiting protein synthesis<sup>16</sup>. Drug-resistant TB needs more prolonged treatment consisting of a combination of second-line drugs such as aminoglycosides (amikacin, kanamycin) with fluoroquinolones (capreomycin)<sup>17</sup>.

## **1.5 Drawbacks of current tuberculosis treatment**

The existing tuberculosis (TB) treatment drugs are systemically distributed throughout the body via oral ingestion or intravenous administration. However, many of these drug molecules tend to accumulate in tissues other than the targeted site, leading to adverse effects such as nephrotoxicity, hepatotoxicity, ocular toxicity, and ototoxicity. Most anti-TB medications are administered orally, resulting in pharmacokinetic challenges such as decreased bioavailability and a narrow therapeutic index. Conventional drug therapy necessitates prolonged regimens involving the frequent and continuous intake of multiple medications, which in turn reduces patient adherence to treatment protocols. Poor adherence to medication is a critical indicator of infection recurrence and the development of multidrug-resistant TB (MDR-TB) and extensively drug-resistant TB (XDR-TB)<sup>11</sup>.

Furthermore, patients often struggle with adherence to conventional pharmacological therapies due to concerns about the duration of treatment, contributing to infectious relapse and the emergence of MDR and XDR-TB. MDR-TB poses a growing challenge to healthcare systems in developing nations. Despite the effectiveness of current anti-TB therapies, there is an urgent need to develop new, shorter treatment regimens incorporating additional drugs to tackle the diverse challenges associated with drug and target selection, as well as patient adherence.

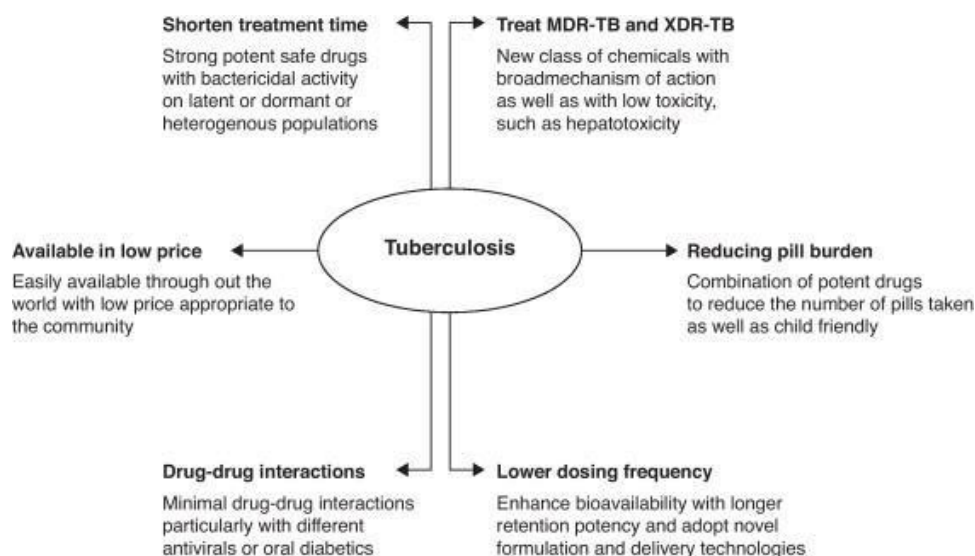


**Figure 1.4:** Schematic diagram representing the desired profile for developing new tuberculosis drugs<sup>6</sup>.

## 1.6 Nanocarrier-based drug delivery in tuberculosis

Given the observations outlined above, it's evident that optimizing tuberculosis (TB) treatment presents a significant challenge. The hypothesis of discovering entirely new active molecules that outperform existing ones appears improbable. Both the scientific and medical communities recognize that research has encountered a discovery void in recent decades. Indeed, the pace of new molecule discovery has significantly decelerated during this period compared to the golden age of antibiotics. Maximizing the potential of existing drugs offers a promising avenue to address many of the aforementioned constraints. The issues with conventional therapeutics have resulted in a paradigm shift to nano carrier-based drug delivery systems.

Advantages of nanosized drug delivery systems can be succinctly summarized as follows:

- I. **Targeted drug delivery:** Nanocarriers facilitate direct delivery of drugs to the infected site, enhancing efficacy and minimizing side effects<sup>18</sup>.

- II. **Enhanced bioavailability:** Nanoformulations improve the solubility of poorly water-soluble anti-TB drugs, enhancing absorption and bioavailability<sup>19,20</sup>.
- III. **Reduced drug dosage:** Efficient delivery and release mechanisms enable therapeutic effects with lower drug doses, reducing side effects and toxicity<sup>19</sup>.
- IV. **Overcoming drug resistance:** Nanocarriers can counter multidrug-resistant TB strains by delivering multiple drugs or protecting drugs from degradation<sup>20</sup>.
- V. **Controlled release:** Drugs encapsulated in nanocarriers are released gradually, maintaining consistent drug levels and potentially reducing dosing frequency<sup>21</sup>.
- VI. **Reduced side effects:** Targeted delivery and reduced dosage minimize exposure of healthy tissues to drugs, thus reducing side effects<sup>19,20</sup>.
- VII. **Improved patient compliance:** Nanosized delivery systems offer simplified dosing regimens, enhancing patient adherence, particularly for TB's lengthy treatment courses<sup>19,20</sup>.
- VIII. **Penetration of biological barriers:** Nanocarriers can traverse tough biological barriers like the blood-brain barrier, facilitating treatment in challenging sites<sup>19</sup>.
- IX. **Protection from degradation:** Some nanocarriers shield drugs from enzymatic or pH-mediated degradation, prolonging drug activity<sup>19</sup>.
- X. **Versatility:** Nanosized delivery systems can transport various drugs, including small molecules, proteins, or nucleic acids, providing flexibility in treatment strategies<sup>19,20</sup>.
- XI. **Co-delivery of multiple drugs:** Certain nanocarriers encapsulate multiple anti-TB agents, enabling more effective combination therapy and reducing the risk of drug resistance<sup>19,20</sup>.

By leveraging these advantages, nanosized drug delivery systems have the potential to revolutionize TB treatment strategies, effectively tackling numerous challenges posed by conventional therapy. Various research groups have explored several nanocarriers for tuberculosis, such as liposomes<sup>22</sup>, niosomes<sup>23</sup>, hydrogels<sup>24</sup>, gold nanoparticles<sup>25</sup>, carbon nanotubes<sup>26</sup>, dendrimers<sup>27</sup>, etc., and various routes of administration of these nanoparticles have also been explored, such as intranasal, intravenous, pulmonary, subcutaneous.

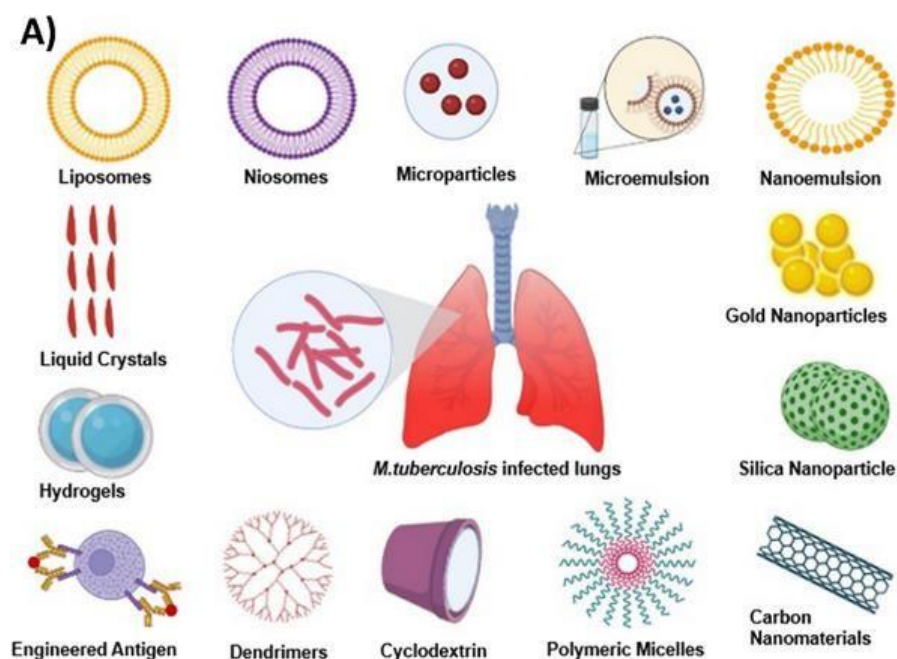


**Figure 1.5:** Various nanoparticles explored for the treatment of tuberculosis<sup>28</sup>.

## 1.7 Metal-organic frameworks

Metal-organic frameworks (MOFs) are porous coordination polymers constructed from a metal ion, also referred to as a node, and an organic ligand, referred to as a linker. It has a crystalline structure with tunable porosity and high surface area. These structures show exceptional chemical and thermal stability. Depending on the organic and inorganic components involved in construction, MOFs can be classified into various types, such as isorecticular MOFs (IRMOF-3), zeolitic imidazolate frameworks (ZIF-7, ZIF-8, ZIF-90, ZIF-L), porous coordination networks

(PCN-333, PCN-224, PCN-57), materials institute Lavoisier (MIL-53, MIL-100), University of Oslo (UiO) MOFs and many more<sup>29</sup>.

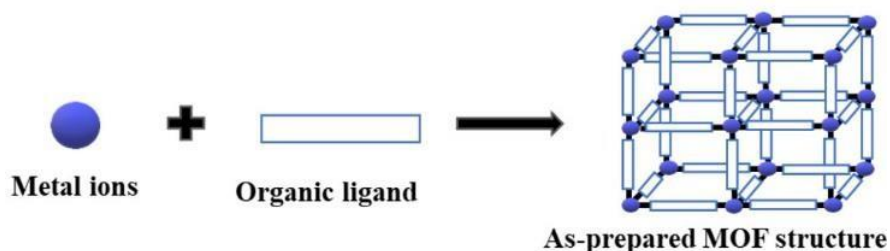


**Figure 1.6:** Formation of MOF structure

In the last few decades, various preparation schemes have evolved and are routinely used to synthesize MOFs. These are the microwave-assisted method, electrochemical synthesis method, conventional solvothermal synthesis method involves high temperature and pressures, mechanochemical method utilizes ball milling and sonochemical method uses high energy sonication. Various factors must be considered during MOF preparation, such as the type of organic ligand and metal ion used. The metal ions serve as a construction node and directly impact the MOF's structure through their coordination geometry. Molar ratios of precursor molecules also play a significant role. Other factors are pH, the type of solvent used, and the temperature of the reaction mixture. Most of these methods use organic solvents such as DMSO, DMF, DEF, EtOH, and MeOH. However, these solvents remain in MOFs post-synthesis and need to be removed through the activation process. To overcome solvent issues and its associated toxicity for biological applications, MOFs are prepared in aqueous conditions<sup>30</sup>.

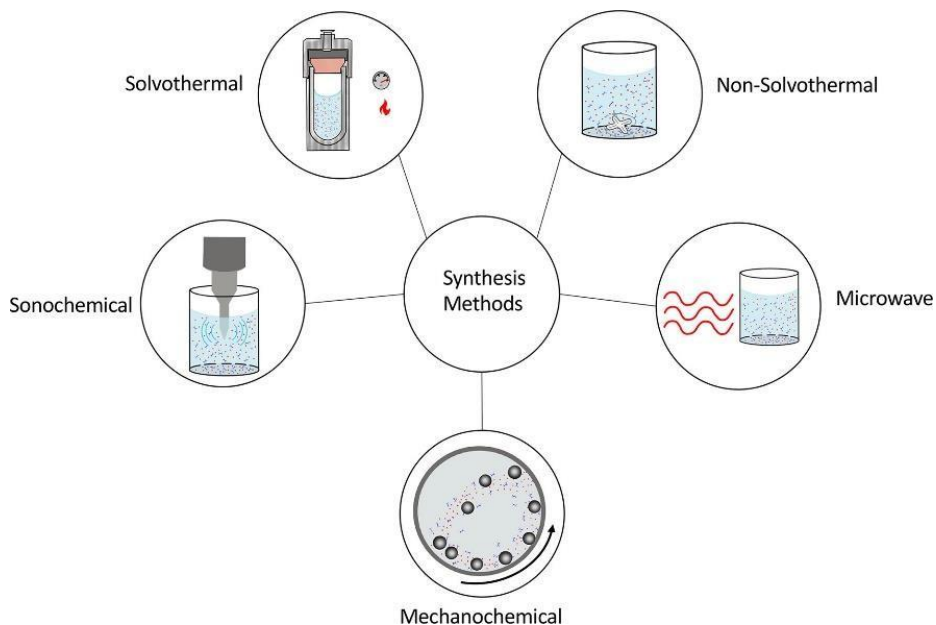


**Figure 1.7:** Methods of MOF synthesis<sup>29</sup>.

Metal-organic frameworks have emerged as promising materials in a variety of fields such as sensors, catalysis, drug delivery, pesticides, biological markers, gas storage and delivery, and wastewater treatment due to their high surface area, structural flexibility, tunable porosity, small density, and easy surface medication and various other properties that are mentioned in figure.

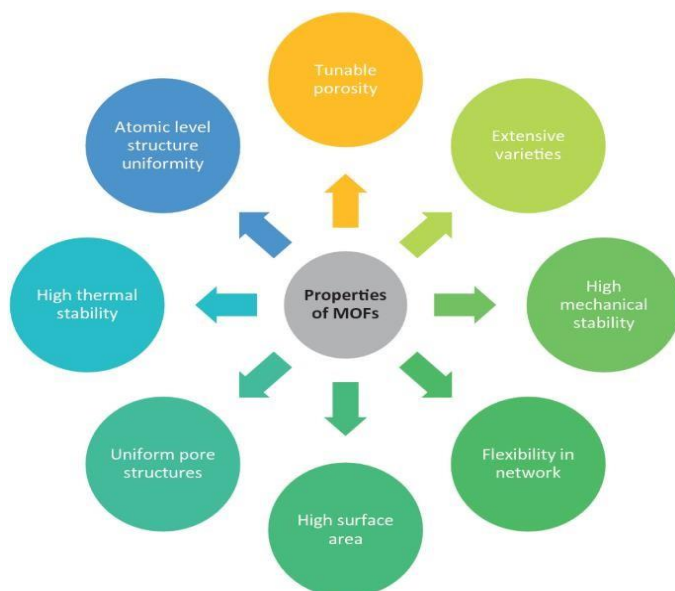


**Figure 1.8:** Properties of MOF<sup>31</sup>.

## **1.8 Applications of metal-organic frameworks in drug delivery**

One of the key applications of MOFs is drug delivery, which allows MOFs to work as carriers of active compounds through the body. Examples of conventional drug delivery systems are tablets, capsules, granules, ointments, syrups for oral use, and suppositories or solutions for intravenous delivery. However, conventional methods are unable to achieve sustained release due to a number of drawbacks and restrictions, such as poor absorption for target sites, repeated dosage several times per day, requirement of high drug dose, fluctuations in plasma drug level, difficulty monitoring drug levels, poor bioavailability issues, critical toxicities, side effects, and premature excretion from the body. MOFs can be used to circumvent many of the above problems. It provides the following advantages: high drug-loading capacities, controlled release and stimuli-responsive release of therapeutics, protection and stabilization of therapeutics in biological environment, adjustable pore size and straightforward surface modification. They are especially useful for encapsulating poorly water-soluble therapeutics<sup>30,32</sup>.

The method used for drug loading is critical for maximizing loading. There are four main methods for drug loading in MOFs: one-pot synthesis, post-synthetic encapsulation, surface loading and biomimetic mineralization. In one-pot synthesis, the drug molecule and the MOF coprecipitate during the synthesis process. As a result, the drug molecules are distributed evenly across the MOF's mesopores. Proteins and nucleic acids, which are examples of biomolecular therapies, can be loaded using biomimetic mineralization.

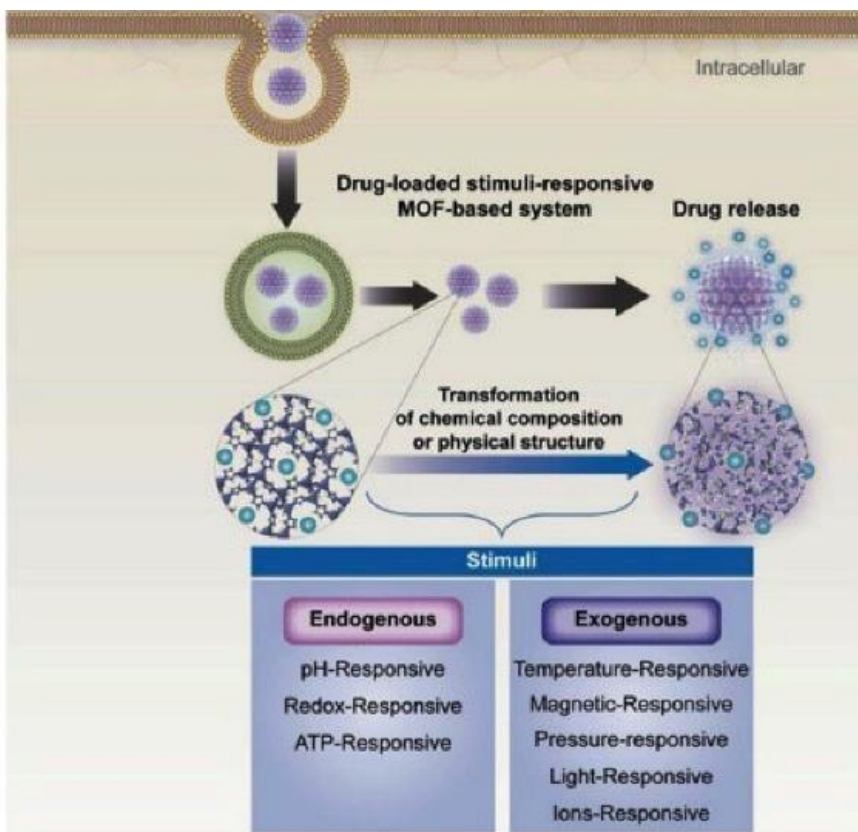


**Figure 1.9:** MOF-based stimuli-responsive system for drug delivery<sup>33</sup>.

Biomimetic mineralization mixes biomolecules and MOF base units in a single reaction mixture, much like one-pot synthesis does. In post-synthetic encapsulation, therapeutic molecules are loaded inside the pores of MOFs after synthesis by mixing the MOF and the drug in a solvent, followed by removal of solvent via evaporation. The excess drug is then removed through washing. Surface loading is mainly governed by electrostatic interactions but can also be achieved by directly linking the drug molecules to the surface. However, this method leads to reduced drug loading and burst drug release<sup>29,32</sup>.

## **1.9 Organisation of thesis**

**1.9.1 Chapter 1** introduces the thesis topic, the prevalence of tuberculosis and its pathogenesis, treatment and its drawbacks, then the discussion turns to nanocarriers and how they will be useful for treatment of tuberculosis especially metal-organic frameworks.

**1.9.2 Chapter 2** provides with an in-depth literature review of use of metal-organic frameworks for treatment of bacterial infections and the success of ZIF-8 as drug delivery system.

**1.9.3 Chapter 3** outlines the thesis objectives

**1.9.4 Chapter 4** outlines the materials and methodologies used to perform successful encapsulation and characterization via techniques such as UV-Vis Spectroscopy, PXRD, FT-IR, TGA and BET as well as discusses methods of in-vitro studies such as cellular cytotoxicity via MTT assay, in-vitro drug release assay and cellular uptake assay

**1.9.5 Chapter 5** is about the results and the discussion of each experiment conducted.

**1.9.6 Chapter 5** is about conclusion made from entire thesis and future directions.



## Chapter 2

### Literature Review

---

#### 2.1 Overview

Antibiotic resistance poses a significant challenge to global healthcare, reducing the effectiveness of treatments and threatening public health. Bacterial pathogens have developed mechanisms to evade immune responses and resist antibiotic action, particularly when residing within host cells. The hydrophilic nature of common antibiotics limits their ability to penetrate cell membranes and eliminate intracellular bacteria, contributing to therapeutic inefficacy and the emergence of resistance. Over the past two decades, nanomedicine platforms have been explored to enhance drug accumulation within infected cells, offering potential advantages for combating intracellular pathogens. Among these platforms, porous coordination polymers, or metal-organic frameworks (MOFs), have emerged as promising drug delivery systems for antibacterial agents.

#### 2.2 Antibacterial mechanisms of MOF-based nanomedicines

MOF-based nanomedicines offer diverse strategies for achieving antibacterial effects. Firstly, MOFs can serve as reservoirs for metal ions with toxic properties for intracellular bacteria, releasing them upon controlled degradation. Various metals, including  $\text{Ag}^+$ ,  $\text{Cu}^{2+}$ , and  $\text{Fe}^{3+}$ , exhibit antibacterial activity through distinct mechanisms. Secondly, MOFs containing bioactive linkers, such as antibiotics or natural antibacterial agents, show potential for multi-bactericidal systems, enhancing efficacy through synergistic effects. Additionally, photosensitizer molecules can be incorporated as organic linkers in MOF structures, enabling photodynamic therapy (PDT) to generate reactive oxygen species (ROS) for antibacterial action. Furthermore, MOFs can function as drug delivery systems (DDS) for antibacterial agents, with

their porous networks enabling encapsulation of antibiotics, antibacterial gases, photosensitizers, and photothermal molecules. Co-delivery of multiple agents within MOFs offers synergistic therapeutic effects. However, noncovalent entrapment may lead to premature drug release, necessitating covalent post-synthesis attachment to improve drug stability. Overall, MOF-based materials provide a versatile platform for designing antibacterial nanomedicines with combined antimicrobial effects<sup>32</sup>.

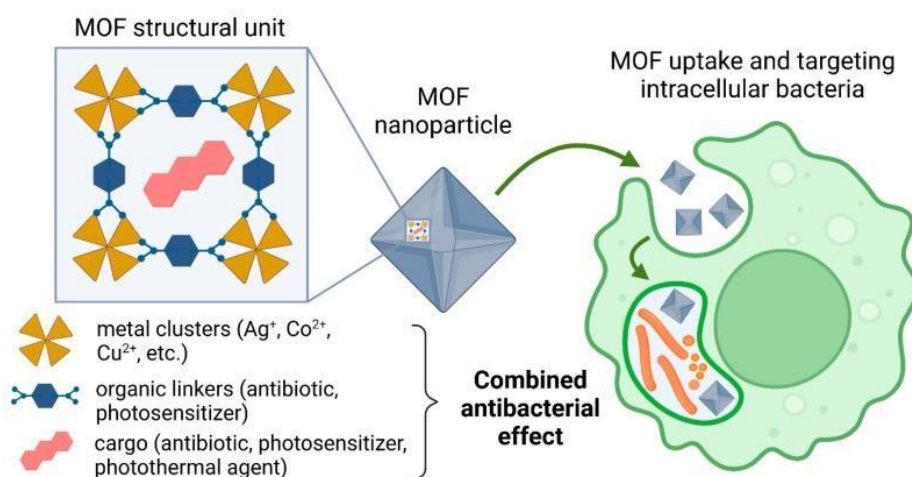


**Figure 2.1:** MOF-based treatment of intracellular infection

Zhang et al. have developed a pH-responsive metal-organic framework (MOF)/antibiotic system to efficiently target and eliminate intracellular bacteria. The system, termed Tet@ZIF-8@hyaluronic acid (TZH), was designed to penetrate biological cell membranes using hyaluronic acid (HA) as a mediator, achieving targeted bacterial eradication while reducing the antibiotic dosage. Through experiments conducted on *Escherichia coli* and *Staphylococcus aureus* bacterial cells, the study demonstrated the effectiveness of TZH in responding to intracellular bacterial infections. The system exhibited satisfactory stability and low toxicity, offering a promising approach to rejuvenate traditional antibiotics and combat antibiotic resistance. This innovative platform holds the potential for revitalizing the efficacy of conventional antibiotics and contributing to the ongoing fight against antibiotic-resistant bacteria<sup>35</sup>.

Simon et al. demonstrated the encapsulation of the anti-tuberculosis medication isoniazid (INH) into MIL-100(Fe) nanoparticles with a 13% drug loading capacity. These INH@MIL-100(Fe) nanoparticles exhibited sustained drug release over 24 hours in phosphate-buffered saline (PBS), with approximately 60% of the drug released without a burst release<sup>36</sup>. Additionally, Uthappa et al. developed a hybrid combination of natural diatom biosilica microparticles loaded with MIL-100(Fe) nanoMOFs, showing a two-fold higher loading capacity for INH and more sustained drug release compared to INH-loaded MIL-100(Fe) nanoMOFs alone. These studies suggest that MIL-100(Fe) is a promising drug delivery platform for INH.

Zeolitic imidazolate frameworks (ZIFs) are an important category of MOFs with highly desirable properties such as high porosity, exceptional thermal and mechanical stability, the pore size of ZIFs is easily tunable which allows in adjustable molecular diffusion/mass transfer and loading of large cargoes, thus making ZIFs excellent candidates for drug delivery applications. ZIF-8 has been successfully used as a drug delivery system for wide range of biomedical application such as for cancer therapy<sup>37</sup>, antibacterial application and biomimetic mineralization.

Sun et al. demonstrated the potential of ZIF-8 for delivering anticancer drugs in vitro. They achieved a remarkable loading of 660 mg of 5-fluorouracil (5-FU) per gram of ZIF-8, with pH-triggered controlled release of the drug. Interestingly, the release rate was significantly faster in acidic conditions (pH 5) compared to neutral conditions (pH 7.4), indicating ZIF-8 as an excellent pH-sensitive drug delivery system (DDS)<sup>38</sup>.

As noted, zeolitic imidazolate frameworks (ZIFs) have the capability to encapsulate a wide range of organic and inorganic cargoes by growing around them, while preserving their functionality. ZIFs have been effectively utilized to encapsulate antibiotics including ciprofloxacin<sup>39</sup>, gentamicin<sup>40</sup>, physcion<sup>41</sup>, ceftazidime<sup>42</sup>, and vancomycin<sup>43</sup> for antimicrobial therapy.



## **Chapter 3**

### **Objectives of the Thesis**

---

#### **3.1 Synthesis and characterization of Zeolitic Imidazolate Framework-8 (ZIF-8)**

For the purpose of drug delivery, the ZIF-8 was synthesized in an aqueous system. The synthesized ZIF-8 was confirmed using PXRD, FTIR and SEM.

#### **3.2 Encapsulation of rifampicin within ZIF-8 and its characterization**

Rifampicin was encapsulated into ZIF-8 post-synthesis, and the encapsulation was confirmed using UV-visible spectroscopy, SEM, EDS analysis, thermal stability, and surface area analysis. pH-responsive release of rifampicin from ZIF-8 was also checked.

#### **3.3 *In-vitro* studies of RIF@ZIF-8**

Cytotoxicity and cellular uptake of ZIF-8 encapsulated with rifampicin (RIF@ZIF-8) was performed in mouse macrophage, RAW 264.7 cell line.



## Chapter 4

### Materials and Methods

---

#### 4.1 Materials

Zinc nitrate hexahydrate ( $\text{Zn}(\text{NO}_3)_2 \cdot 6\text{H}_2\text{O}$ ) of 98% purity was purchased from Sigma Aldrich. 2-Methylimidazole ( $\text{C}_4\text{H}_6\text{N}_2$ ), 99% pure and Rifampicin, cell culture grade, was acquired from Sisco Research Laboratories Pvt. Ltd., 3-(4,5-Dimethylthiazolyl-2)-2,5-diphenyl tetrazolium bromide (MTT) and dimethyl sulfoxide, cell culture reagent was purchased from MP biomedical. Middlebrook 7H9 broth was from BD Difco. Dulbecco's Modified Eagle Media (DMEM), Fetal Bovine Serum (FBS), and 100X Antibiotic-Antimycotic were from Gibco, Thermo Fischer Scientific.

#### 4.2 Synthesis of zeolitic imidazolate framework-8 (ZIF-8)

ZIF8 was synthesized in an aqueous system. The protocol followed was previously reported by Pan et. Al<sup>45</sup>, however, few modifications were made. The molar ratio of components used for synthesis plays an important role in determining the pore size of ZIF8. Molar ratio of zinc nitrate hexahydrate: 2-methylimidazole: water taken was 1:70:1238. In one beaker, 1.17g of zinc nitrate hexahydrate was dissolved in 8 ml of miliQ water and in a separate beaker, 22.70g of 2-methylimidazole was dissolved in 80 ml of miliQ water. The zinc nitrate solution was added dropwise into the imidazole solution, which was kept on a magnetic stirrer. The reaction mixture turned milky. The solution was stirred at 450 rpm for 6 hours at room temperature. After 6 hours the product was collected by centrifugation at 8000 rpm for 10 minutes. The synthesized ZIF-8 was washed 5 times with Milli-Q water to remove unreacted chemicals. The product was dried at 60 °C overnight in a drying oven.

### 4.3 Activation of ZIF-8

ZIF-8 was synthesized in water as a solvent system, so there is a high chance that these water molecules may be present within the MOF and occupy some space within the pores. Thus, decreasing the encapsulation efficiency of the drug. So, MOFs are activated to create a solvent-free and highly porous framework before utilizing it as a drug delivery system<sup>44</sup>. ZIF-8 was activated using the solvent exchange. For the process of solvent-exchange acetone was used as a solvent. ZIF-8 was submerged in acetone for 3 consecutive days, and the acetone was changed twice a day. After three days, the acetone was completely removed and the solvent-exchanged samples were heated under extreme vacuum conditions at 80 °C for 4 hours.

### 4.4 Rifampicin encapsulation within the ZIF-8 framework

To encapsulate rifampicin, activated ZIF-8 nanocrystals were stirred in the rifampicin solution having a concentration of 100 µg/ml prepared in 50 % methanol for 48 hours at room temperature at 300 rpm in the dark. After 48 hours, the rifampicin encapsulated ZIF-8 (RIF@ZIF-8) was collected by centrifugation at 8000 rpm for 10 minutes. Excess rifampicin molecules adhered to the surface of ZIF-8 were removed by washing the product with 50 % methanol three times. The product was kept at room temperature for 2 days for the methanol to evaporate. The Supernatant and the wash solution were stored for the determination of encapsulation efficiency and drug-loading content using a UV-Vis spectrophotometer. A linearity plot of rifampicin in 50 % methanol was constructed and the  $y = mx + c$  equation was used to extrapolate the amount of drug encapsulated. The encapsulation efficiency and drug loading content were calculated according to the formula given below<sup>46</sup>.

$$\begin{aligned} &\text{Drug encapsulation efficiency (DEE)} \\ &= \frac{\text{Quantity of overloaded drug}}{\text{Quantity of feeding drug}} \times 100 \% \end{aligned}$$

## **4.5 Characterization of rifampicin encapsulated ZIF-8 (RIF@ZIF-8)**

There are multiple characterization methods available to confirm successful drug loading. PXRD, FTIR, and NMR are used to check if proper synthesis of MOFs has been done and to check encapsulation. Electron microscopy, such as scanning electron microscopy and transmission electron microscopy, as well as dynamic light scattering, can be used to study the morphology and size of MOFs. UV-Vis spectroscopy, thermogravimetric analysis, and nitrogen adsorption-desorption isotherms are also routinely used to confirm encapsulation.

### **4.5.1 UV-Visible spectrophotometer**

UV-Visible spectroscopy is an analytical technique that measures the absorption or transmission of specific wavelengths of UV or visible light in a sample compared to reference. This property is affected by the sample's composition, providing information on the contents and concentration of the sample (based on Beer-Lambert's law).

UV-Visible spectrophotometer UV-1900i of Shimadzu was used to study the absorption spectra of rifampicin in methanol, prepare the calibration curve, and calculate encapsulation efficiency.

### **4.5.2 Powder X-ray diffraction (PXRD)**

Powder X-ray diffraction is a method mainly used for the characterization of crystalline materials, measurement of sample purity and determination of unit cell dimensions. It is based on constructive interference of monochromatic X-rays and the sample material. The X-rays interact with the sample and produce constructive interference and a diffracted ray when conditions meet Bragg's law. Bragg's law ( $n\lambda=2d \sin \theta$ ) correlates the wavelength of electromagnetic radiation to diffraction angle and the lattice spacing in a crystalline sample. The diffracted X-rays are then

detected and processed. The sample is scanned through a range of  $2\theta$  angles to acquire all possible diffraction directions of lattice.

Rigaku SmartLab, Automated Multipurpose x-ray Diffractometer was used for PXRD analysis of ZIF-8 pre and post activation as well as after encapsulation. 15-20 mg of powdered sample was used to create a thin powder film.  $2\theta$  scan range was from  $2^\circ$  to  $80^\circ$ .

#### **4.5.3 Fourier-transform infrared spectroscopy (FTIR)**

FTIR Spectroscopy, also known as Fourier-transform infrared spectroscopy, examines the molecular vibrations of substances. Each unique functional group within a molecule exhibits distinct vibrational energy, and by analyzing the collective vibrations of all functional groups, it becomes possible to identify the molecule. In infrared spectroscopy, IR radiation passes through a sample. During this process, the sample absorbs some of the infrared energy while the remainder is transmitted through. The resulting spectrum provides a molecular fingerprint for the sample, showcasing its absorption and transmission characteristics. As no two fingerprints are identical, no two unique molecule configurations yield the same infrared spectrum.

FTIR spectra of ZIF-8 and RIF@ZIF-8 was recorded using BRUKER TENSOR 27 FT-IR. All samples were scanned between  $4500\text{-}500\text{ cm}^{-1}$  at a resolution of  $4\text{ cm}^{-1}$ . All scans were performed at room temperature.

#### **4.5.4 Scanning electron microscopy (SEM) and energy dispersive spectroscopy (EDS)**

Scanning electron microscopy (SEM) is a technique that allows for the imaging of surfaces at high resolution using an electron beam. It is based on the interaction between a beam of electrons and a sample surface. The electrons interact with atoms in the sample producing various signals that can be detected and used to form an image. The sample material is irradiated with electrons resulting in emission of x-rays characteristic to the elements present. The EDS detector detects these x-rays and are translated into spectral peaks of varying intensity which is proportional to

the concentration of the element present. SEM is particularly useful for studying surface morphology, particle size, and material composition.

JSM-7610FPlus field emission scanning electron microscope was used to study the morphology and particle size of ZIF-8 and RIF@ZIF-8. Carbon tape was used for sample preparation and the sample was coated with gold via sputter coating for 5 minutes.

#### **4.5.5 Thermogravimetric analysis (TGA)**

Thermogravimetric analysis is a technique that measures the thermal stability of materials. It measures the changes in the mass of the sample as the temperature is increased. A precision balance holds a sample pan in place during a TGA. Throughout the experiment, the pan is heated or cooled while housed in a furnace, and the mass of the sample is tracked. The sample environment is managed by a sample purge gas.

Mettler Toledo TGA/DSC 1 STARe system was used for TGA. For each analysis, approximately 5 mg of sample was loaded and heated from 50 °C to 800 °C at a heating rate of 10 °C/ minute under air flow while the weight was measured and recorded continuously.

#### **4.5.6 Nitrogen adsorption-desorption isotherms**

The Brunauer-Emmett-Teller (BET) technique employs gas physisorption measurement to determine the "surface area" of a sample. Gas molecules penetrate all pores, cracks, and surface irregularities, enabling the complete microscopic surface area assessment. Typically applied to powders or granules, the outcome is expressed as a specific surface area, denoted in units of area per unit mass. Alternatively, it can be represented as area per unit volume or as the absolute area of an object.

The Brunauer-Emmett-Teller (BET) surface area of the pure ZIF-8 and rifampin loaded ZIF-8 particles were determined via N<sub>2</sub> adsorption-desorption isotherm measurement at 77 K (Thermo Scientific, sorptomatic 1990) after degassing at 400 °C for 2 hours.

## 4.6 Cell line and cell culture conditions

RAW264.7, an adherent macrophage cell line, was used for cell viability and intracellular survival experiments. RAW264.7 cells were acquired from the National Centre for Cell Science, India. The cells were cultured in Dulbecco's modified eagle medium supplemented with 10% fetal bovine serum in a humidified atmosphere with 5% CO<sub>2</sub> at 37 °C (CO<sub>2</sub> incubator).

## 4.7 *In-vitro* drug release assay

The purpose of using ZIF-8 as a vehicle for the delivery of rifampicin was because of the pH-responsive degradation of ZIF-8. At acidic pH, the ZIF-8 is dissociated. The dissociation occurs by the detachment of the coordination bonds between Zn metal ions and organic imidazole ligands. This leads to the destruction of the ZIF8 structure and increases rifampicin release from RIF@ZIF-8. Thus, the RIF@ZIF-8 system, with pH-dependent drug release, is promising for use as a drug carrier and to target mycobacterium infections, as the pH of infected cells is lower, causing increased drug release only once engulfed by infected cells<sup>47</sup>.

pH-responsive drug release from ZIF-8 was studied at three different pHs, i.e., pH 7.4 (physiological pH), pH 6.5, and pH 5.8 (lysosomal pH) at 37 °C. Synthesized RIF@ZIF powder was weighed and dispersed in 20 ml of PBS buffer of respective pH and kept in the dark, followed by incubation in shaking condition (37 °C, 150 rpm). 1 ml of released solutions was taken out at predetermined time points, and a UV-Vis spectrophotometer was used to determine the percentage of release of rifampicin in comparison to the standard curve of free rifampin at regular time intervals.

## 4.8 Cell viability studies

To check the biocompatibility of ZIF-8, RIF@ZIF-8, and rifampicin alone, cell viability studies were performed using MTT assay. The MTT assay is utilized to gauge cellular metabolic activity as an indicator of cell health, growth, and potential toxicity. This method relies on a colorimetric process where a yellow tetrazolium salt (known as MTT or 3-(4,5-dimethylthiazol-

2-yl)-2,5-diphenyltetrazolium bromide) is transformed into purple formazan crystals by metabolically active cells. These active cells possess NAD(P)H-dependent oxidoreductase enzymes, which facilitate the reduction of MTT to formazan. Following this reaction, the formazan crystals are made soluble using a specific solution, resulting in a colored solution whose intensity is measured by its absorbance at 500-600 nanometres using a multi-well spectrophotometer.

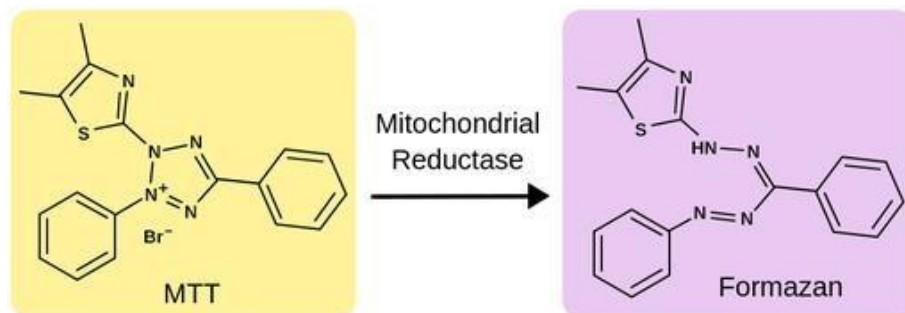


**Figure 4.1:** Chemical reaction of MTT assay

A darker solution indicates a higher concentration of viable, metabolically active cells. In a 96-well plate, 10,000 RAW 264.7 cells were seeded in each well and incubated in a CO<sub>2</sub> incubator for 24 hours. After 24 hours, cells were incubated with MOFs and drugs at concentrations of 2, 5, 10, 20, 30, 40, 50, 80, and 100 µg/ml for each ZIF-8, RIF@ZIF-8, and rifampicin alone (based on loading content) for 24 hours. After 24 hours, the media was discarded, and new media containing MTT at a concentration of 0.1 mg/ml was added to each well and kept in a CO<sub>2</sub> incubator for 4 hours. After 4 hours, the MTT-containing media was discarded, and 200 µl of dissolving solution (11g of SDS dissolved in 50 ml of 0.02M HCl and volume made up to 100 ml using isopropanol.) and the plate was incubated for 30 minutes in a CO<sub>2</sub> incubator. After 30 minutes, the solution was mixed properly using a pipette, and absorbance was recorded using a microplate reader at 570 nm.

## 4.9 Cellular uptake assay

It is important to determine whether the RIF@ZIF-8 synthesized is able to enter the cells because the drug needs to be released inside the cell. Hence, it is important to the cellular uptake of RIF@ZIF-8.

$5 \times 10^4$  mouse macrophage, RAW 264.7, cells were seeded in 24 well tissue culture plates containing coverslips. Post 60-70% confluency, the cells were treated with RIF@ZIF-8 at 5  $\mu\text{g/ml}$  concentration. The cells were incubated for respective time points, i.e., 2 hours and 48 hours. After the respective timepoint incubation the cells were fixed with methanol and acetone mixture (1:1 ratio) and incubated at -20 degrees Celsius for 20 min. Afterward, the cells were washed 3 times with 1xPBS and mounted on grease-free glass slides using antifade DAPI with mounting solutions. The slides were then observed and analyzed using a BX61 Olympus fluorescence microscope.

## Chapter 5

### Results and Discussion

---

#### 5.1 Characterization of synthesized ZIF-8 via powdered X-ray diffraction (PXRD)

A PXRD study was performed to check if the ZIF-8 that was synthesized was formed correctly. PXRD is widely used for the identification of crystalline structures, as each crystalline material gives unique peaks. According to the literature<sup>48</sup> ZIF-8 gives characteristic diffraction peaks at  $2\theta$ :  $7.4^\circ$ ,  $10.4^\circ$ ,  $12.7^\circ$ ,  $14.7^\circ$ ,  $16.4^\circ$ ,  $18.0^\circ$ ,  $22.1^\circ$ ,  $24.5^\circ$ ,  $26.7^\circ$  and  $29.6^\circ$  which can be assigned to its planes that is (011), (002), (112), (022), (013), (222), (114), (233), (134) and (044) planes respectively. As seen in figure 5.1, the synthesized ZIF-8 showed all these characteristic peaks at its respective planes, suggesting that the ZIF-8 was synthesized accurately.

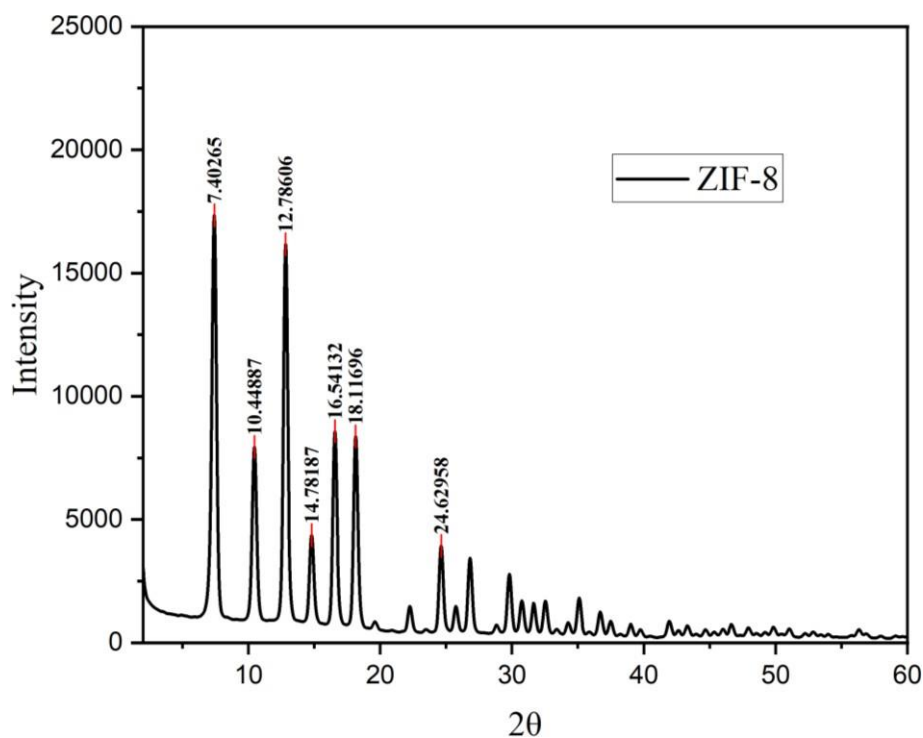


**Figure 5.1:** PXRD spectra of synthesized ZIF-8

## 5.2 Characterization of synthesized ZIF-8 via Fourier-transform infrared spectroscopy (FTIR)

The chemical structure and functional groups present in the synthesized ZIF-8 were analyzed using FTIR spectroscopy. The FTIR Spectroscopy revolves around molecular vibration, where each functional group possesses distinct vibrational energy. This characteristic energy can be employed to discern a molecule by considering the collective contribution of all functional groups. ZIF-8 showed significant peaks at 3135, 2929, 1585, 1458, 1309, 1146, 995, 760, 694 and 426  $\text{cm}^{-1}$ . These FTIR peaks were consistent with those previously reported in the literature. The peaks at 3135 and 2929  $\text{cm}^{-1}$  were due to the aromatic and aliphatic C–H asymmetric stretching vibrations, respectively, of the imidazole ring and methyl group present in the linker. The peak at 1585  $\text{cm}^{-1}$  corresponded to the C=N stretching vibration mode, whereas the peaks from 1460 to 1309  $\text{cm}^{-1}$  corresponded to entire ring stretching. The peak at 1146  $\text{cm}^{-1}$  was associated with aromatic C–N stretching mode. The peaks at 995 and 760  $\text{cm}^{-1}$  were due to C–N bending vibration and C–H bending mode, respectively. The peak at 694  $\text{cm}^{-1}$  was due to the ring out-of-plane bending vibration of the 2-methylimidazole. An intense Zn–N stretching vibration peak was observed at the position of 426  $\text{cm}^{-1}$ , suggested that zinc ions combined chemically with nitrogen atoms of the methylimidazole groups to form the imidazolate during ZIF-8 synthesis<sup>48</sup>.

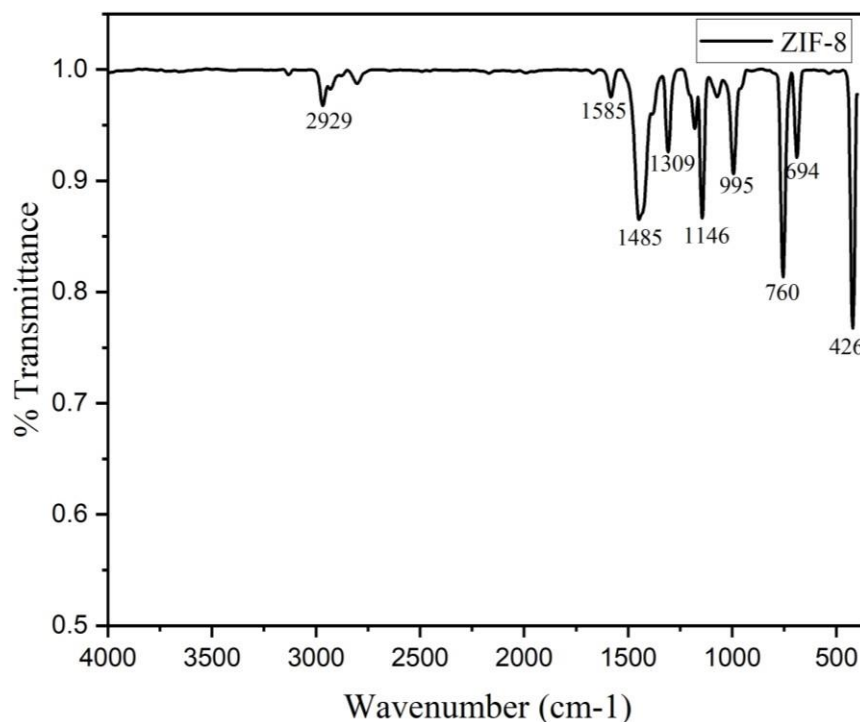


**Figure 5.2:** FTIR spectra of ZIF-8

### 5.3 Activation of ZIF-8

ZIF-8 was produced in a water-based solvent system, raising the possibility of solvent molecules being trapped within the framework and filling some of the pores. Therefore, to achieve a solvent-free and exceptionally porous structure suitable for drug delivery purposes, we activated the ZIF-8 prior to its use as a carrier. This activation process involved conducting a solvent exchange experiment on the synthesized material. Simply heating the MOF under vacuum conditions to remove solvent may collapse the framework. Framework collapse due to high surface tension and capillary forces imposed on structure by liquid-to-gas phase transformation of a trapped solvent when the solvent has a high boiling point/ high surface tension<sup>49,50</sup>. To avoid the problems of framework collapse, before activation, the solvent was exchanged with lower boiling point/lower-surface tension solvent such as acetone.

After activation, the XRD spectra of ZIF-8 was taken. As seen in the figure. All the characteristic diffraction peaks were observed suggesting that after activation, the structural integrity of ZIF-8 was maintained.

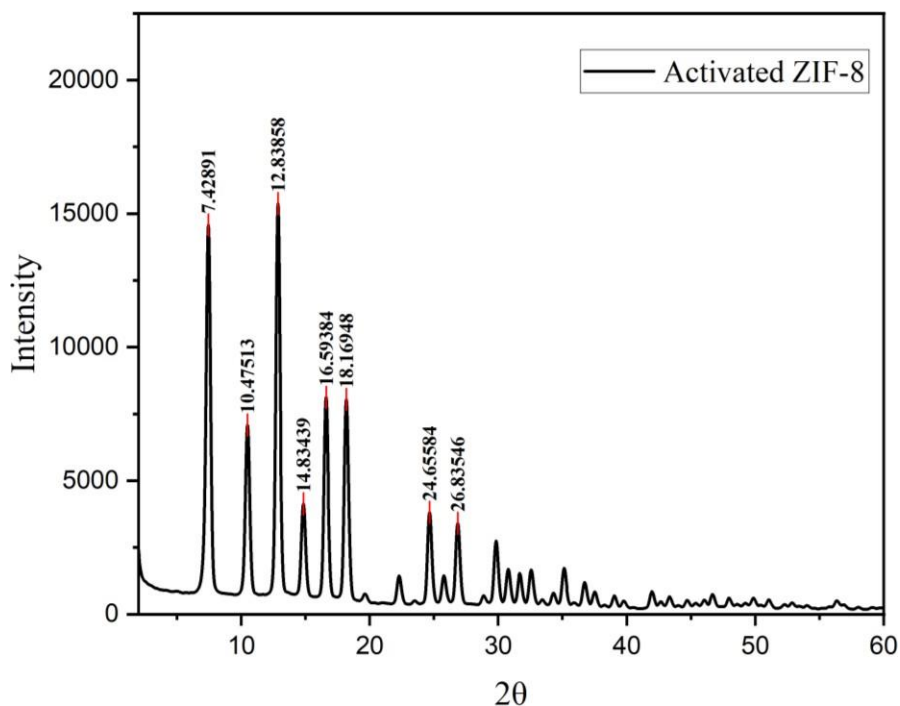


**Figure 5.3:** PXRD spectra of ZIF-8 after activation

#### **5.4 Encapsulation of rifampicin in ZIF-8 (RIF@ZIF-8)**

The absorption spectra of rifampicin in methanol was to determined to figure out the wavelength at which rifampicin absorbs maximum in methanol as a solvent. As seen in the figure, rifampicin show two major peaks, one at 337 nm and other at 477 nm. The absorption maxima of rifampicin is 337 nm so this wavelength was used for further analysis.

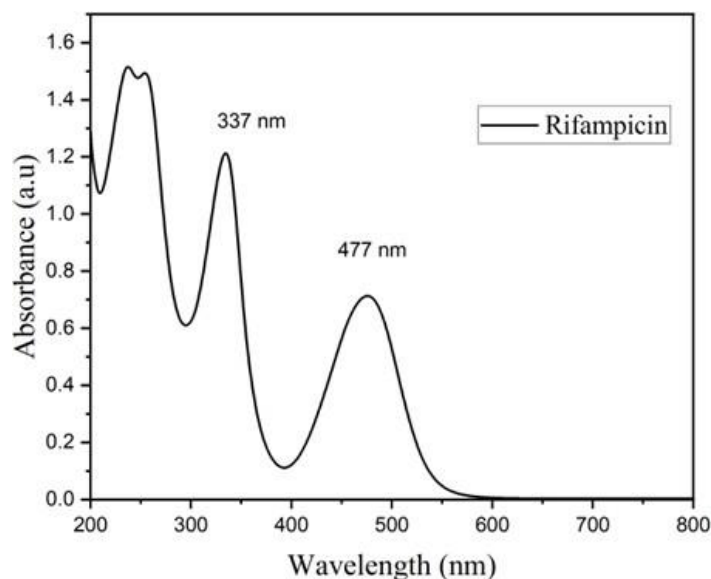


**Figure 5.4:** Absorption spectra of rifampicin

Calibration curve was prepared by making different concentrations of rifampicin and its absorbance was noted. Based on the linearity coefficient and regression equation provided by calibration curve, the unknown concentration of rifampicin in the supernatant was calculated. Based on the calibration curve and the formula of encapsulation efficiency given in the methods section. The encapsulation efficiency was calculated. The encapsulation efficiency was 82 %.

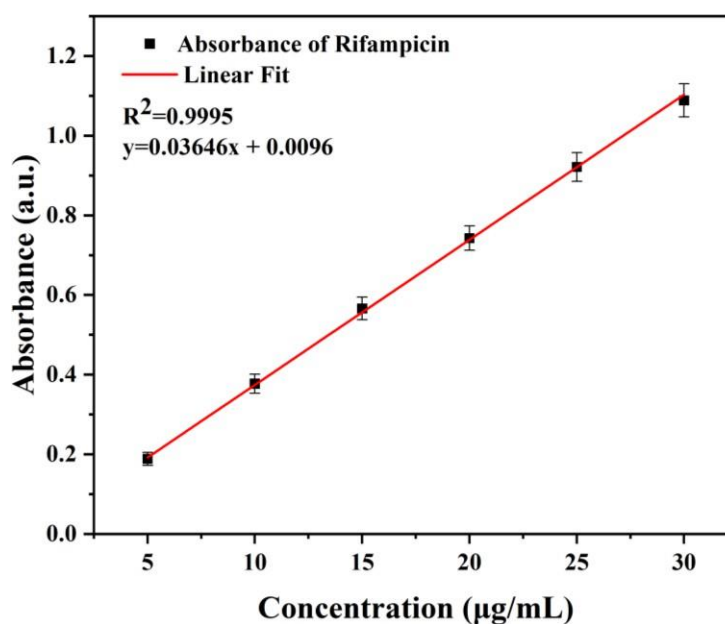


**Figure 5.5:** Calibration curve of rifampicin

## 5.5 Confirmation of encapsulation using UV-Vis spectroscopy

To ensure that the drug was encapsulated in ZIF-8, UV-Vis spectra of rifampicin, ZIF-8 and RIF@ZIF-8 was checked. Rifampicin absorbed maximum at 337 nm, this peak was absent in ZIF-8, whereas a peak at 320 nm was observed in the case of RIF@ZIF-8. There is a blue shift in the absorbance peak of rifampicin present in RIF@ZIF-8. This indicated successful encapsulation of rifampicin in ZIF-8 crystals.

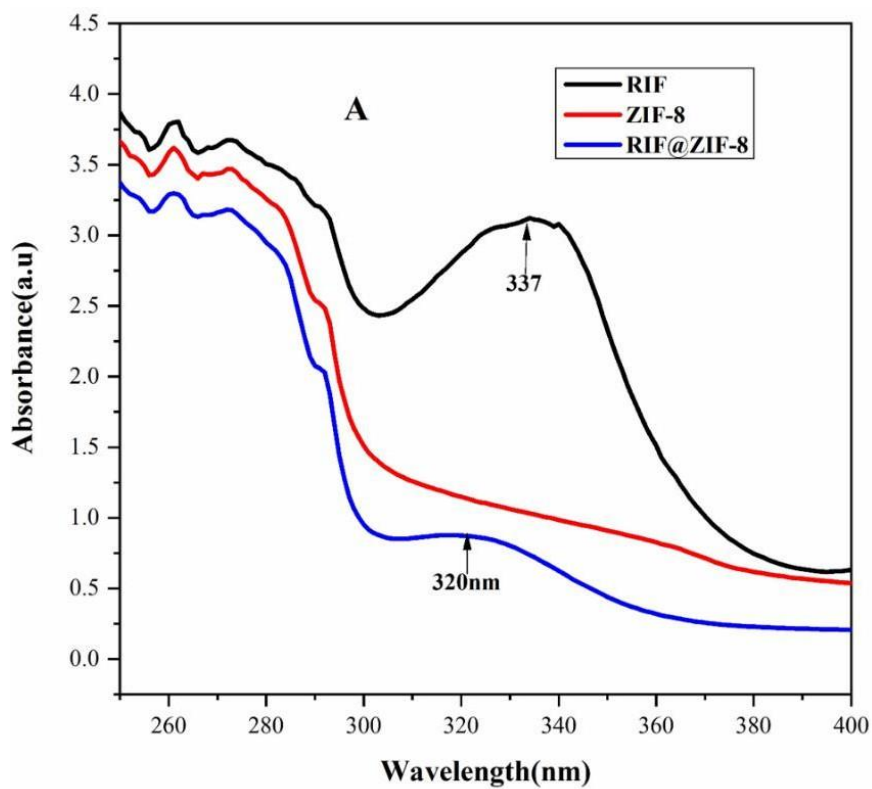


**Figure 5.6:** UV-visible spectra of RIF, ZIF-8, and RIF@ZIF-8

## 5.6 Morphology and surface analysis using scanning electron microscopy (SEM) and energy dispersive X-ray spectroscopy (EDS)

SEM and EDS analysis were used as an additional tool to determine whether the sample was phase pure, to confirm the morphology of ZIF-8 post-synthesis and post-encapsulation, and to evaluate particle size. From the SEM images, it can be clearly observed that both ZIF-8 (figure 5.7) and RIF@ZIF-8 (figure 5.8) showed the hexagonal shape characteristic of ZIF-8 nanoparticles according to the previous literature<sup>45</sup>. The average particle size of ZIF-8 was 110 nm. Elemental mapping analysis showed an even distribution of zinc, carbon, and nitrogen elements. This is consistent with previous literature<sup>51</sup>.

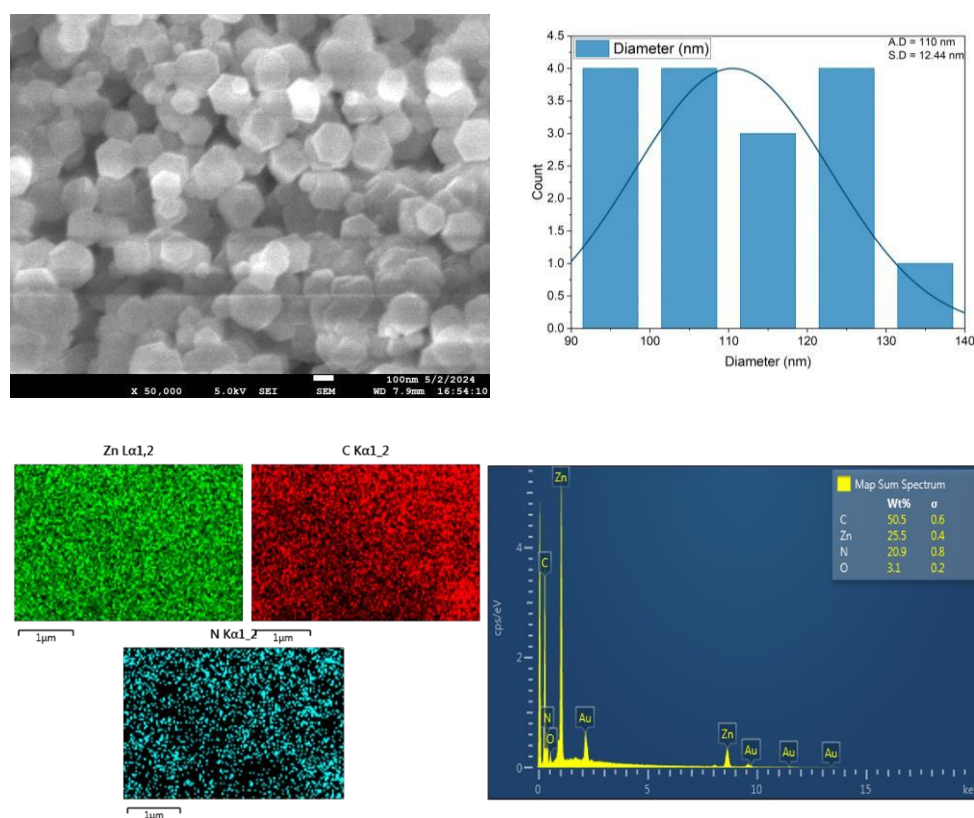
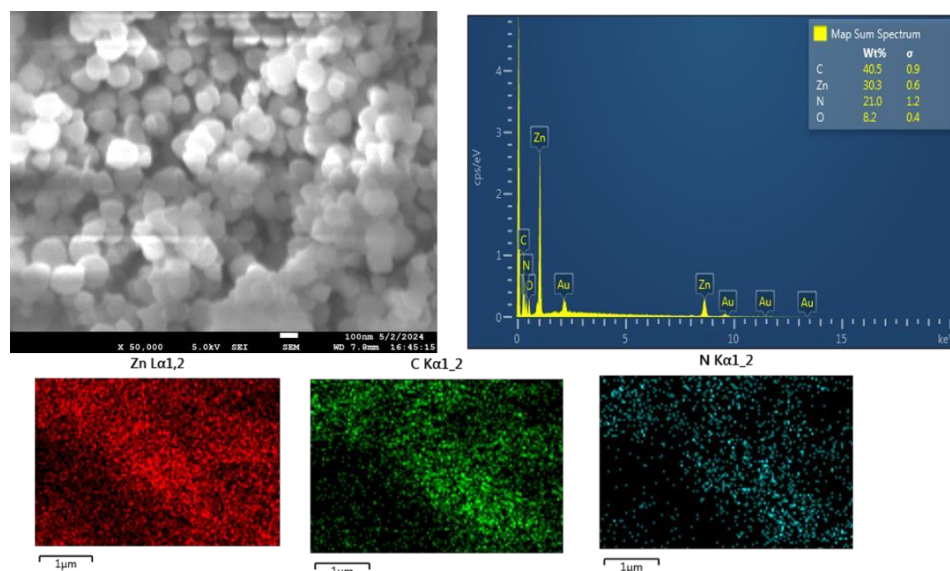


Figure 5.7: SEM and EDS analysis of ZIF-8

After the encapsulation of ZIF-8 with rifampicin, the characteristic hexagonal shape of ZIF-8 was maintained, suggesting that the encapsulation process did not distort the morphology of nanoparticles. Elemental mapping analysis showed an even distribution of zinc, carbon, and nitrogen elements.



**Figure 5.8:** SEM and EDS analysis of RIF@ZIF-8

### 5.7 Thermal stability analysis of ZIF-8 and RIF@ZIF-8

Thermogravimetric analysis was performed to determine the thermal stability of ZIF-8 and RIF@ZIF-8. ZIF-8 was thermally stable till 520 °C and RIF@ZIF-8 was stable till 460 °C. However, after those respective temperatures, the frameworks showed significant decomposition. However, the RIF@ZIF-8 framework had started melting from around 180 °C because of the presence of rifampicin. Therefore, the encapsulation of rifampicin is clearly evident from the thermal stability profile of RIF@ZIF-8.

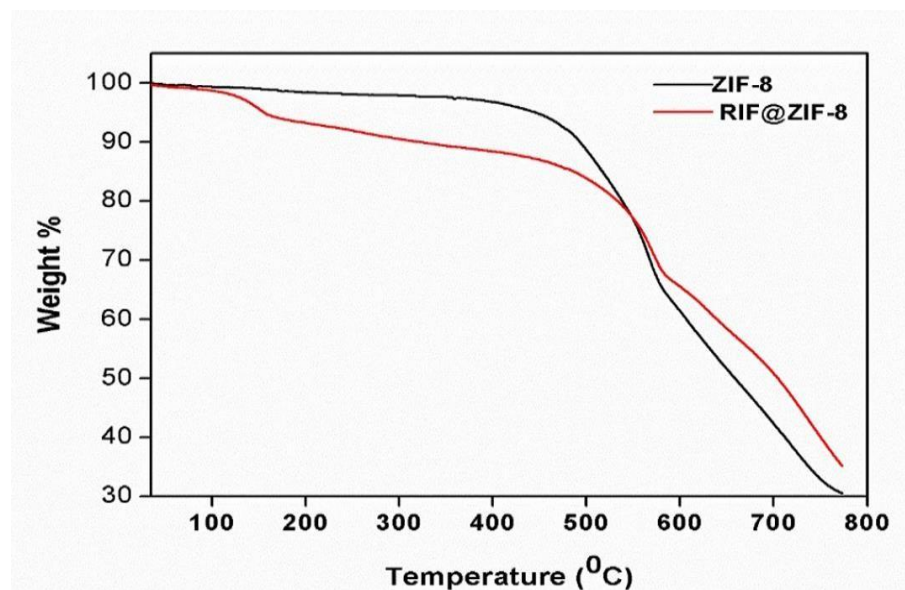


**Figure 5.9:** TGA Analysis of ZIF-8 (black line) and RIF@ZIF-8 (red line)

### 5.8 Surface area analysis of ZIF-8 and RIF@ZIF-8

Brunauer-Emmett-Teller (BET) adsorption studies were performed to confirm that rifampicin was encapsulated in ZIF-8, the nitrogen adsorption-desorption isotherms of pure ZIF-8 and RIF@ZIF-8 were measured at 77K. A significant increase in nitrogen uptake during adsorption experiments at low relative pressures suggested high microporosity of ZIF-8 and RIF@ZIF-8.

The BET surface areas of pure ZIF-8 and RIF@ZIF-8 were 1853.06 m<sup>2</sup>/g and 1333.147 m<sup>2</sup>/g, respectively. The resulting decrease in the surface area of RIF@ZIF-8 compared to ZIF-8 suggested the presence of rifampicin in ZIF-8.

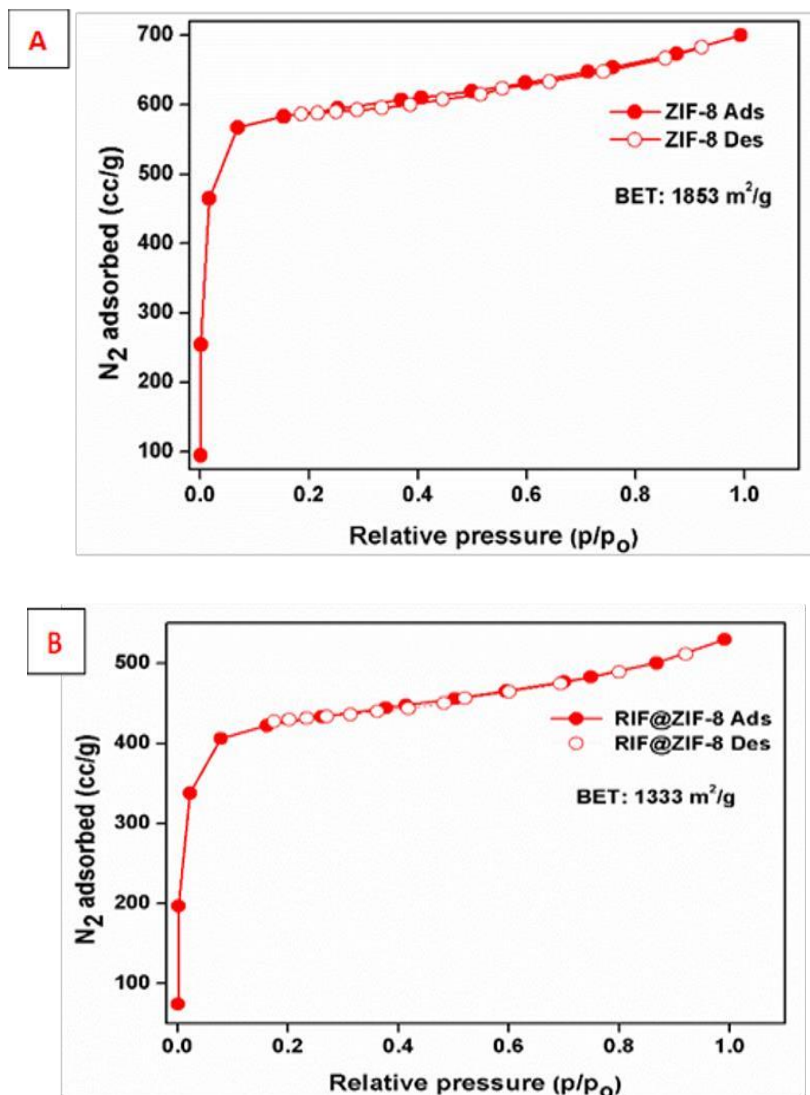


**Figure 5.10:** Nitrogen Adsorption isotherm of ZIF-8 (A) and RIF@ZIF-8 (B)

### 5.9 In-vitro pH-responsive release of rifampicin from RIF@ZIF-8

Rifampicin was encapsulated into ZIF-8 for sustained drug release and to increase its bioavailability. ZIF-8 nanocrystals are known to remain stable at physiological pH 7.4 and disintegrate under acidic conditions. Hence, the pH-dependent drug release profile of rifampicin was studied using an in-vitro release assay. It is known from the literature that infected macrophages are slightly acidic in nature when compared to healthy cells. Therefore, the drug release was checked at three different pHs, i.e., pH 7.4, 6.5, and 5.8. As seen in figure 5.11, RIF@ZIF-8 shows a slow release

of rifampicin at physiological pH 7.4 as compared to acidic pH 6.5 and 5.8. The drug was stably released for 7 days. Approximately 40% of rifampicin was released at an early timepoint with pH 7.4, whereas 59% and 66% of rifampicin were released at pH 6.5 and 5.8, respectively. This suggests that there is a burst release of rifampicin at an early time point in acidic pH that will be likely encountered in infected macrophages. At acidic pH of 6.5 and 5.8, 95% of the drug was released by 4 days, whereas in the case of physiological pH 7.4, only 82% of the drug was released by 4 days.

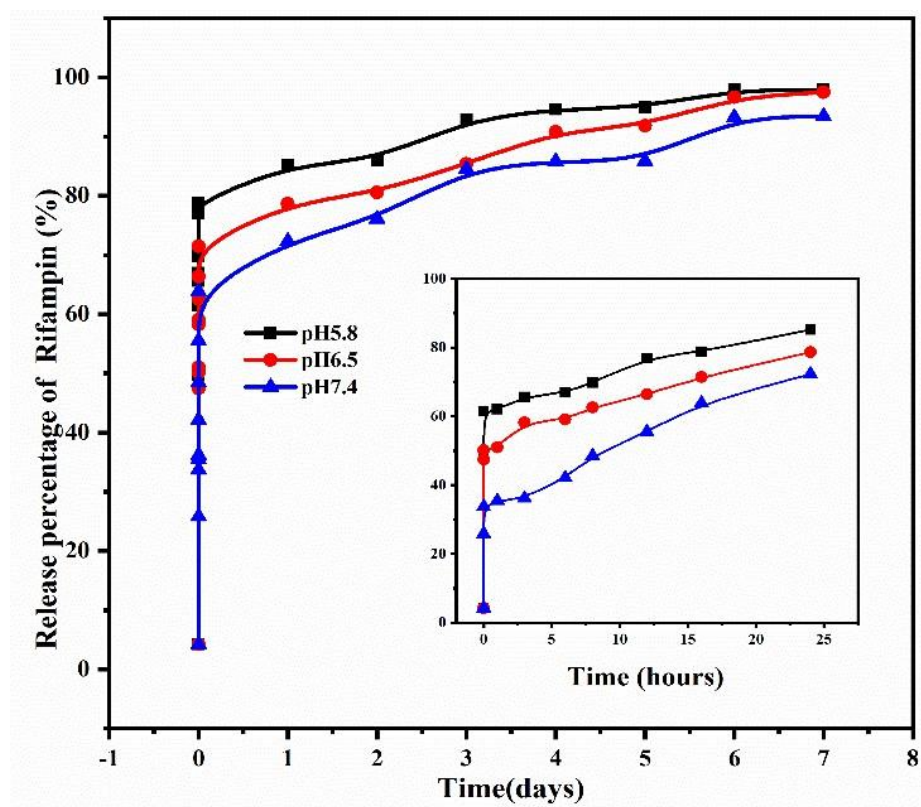


**Figure 5.11:** Drug release profile of rifampicin from RIF@ZIF-8 at three different pH. The main graph represents release % along days whereas the small insert graph represents release % along hours.

### 5.10 *In-vitro* cytotoxicity study of RIF@ZIF-8

Cytotoxicity of ZIF-8, RIF@ZIF-8 and RIF were checked on RAW 264.7 cells using MTT assay. Before using RIF@ZIF-8 for any further in-vitro and in-vivo studies, it is important to check its toxicity. RAW 264.7 macrophages were exposed to a wide range of concentrations ranging from 0 to 100  $\mu\text{g/ml}$  of ZIF-8 and RIF@ZIF-8, whereas the concentration used for only rifampicin was based on loading content (LC) of rifampicin into RIF@ZIF-8. The macrophages were exposed to ZIF-8, RIF@ZIF-8 and rifampicin for 24 hours. ZIF-8 and RIF@ZIF-8 showed good biocompatibility till 40  $\mu\text{g/ml}$  as more than 80 % cell viability was observed till that concentration. However, the cell viability decreased as the concentration was increased as at 100  $\mu\text{g/ml}$  the cell viability was zero. Therefore, for further studies, RIF@ZIF-8 can be used till a concentration of 40  $\mu\text{g/ml}$  without any toxicity.

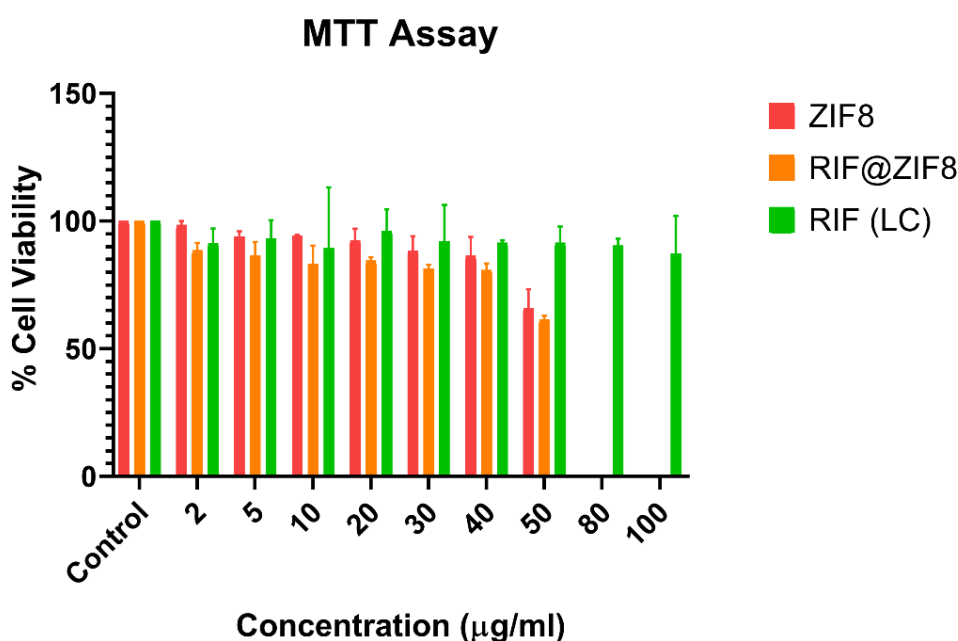


**Figure 5.12:** Cell viability of ZIF-8, RIF@ZIF-8, and rifampicin at a concentration range of 0 to 100  $\mu\text{g/ml}$ . Rifampicin alone was added based on loading content.

## 5.11 Cellular uptake of RIF@ZIF-8

To investigate the cellular uptake of RIF@ZIF-8 by macrophages, fluorescence microscopy was done using RAW 264.7 cell line. RAW 264.7 macrophages were treated with RIF@ZIF-8 for 2 and 48 hours. As seen in the figure, RIF@ZIF-8 was endocytosed by macrophages within 2 hours of incubation. The blue fluorescence is due to DAPI staining of nuclei, whereas the red fluorescence is due to RIF@ZIF-8 nanoparticles. It is important to note that even after 48 hours, the nuclei did not show any fragmentation, indicating that RIF@ZIF-8 did not show apoptosis. Thus, RIF@ZIF-8 can successfully enter macrophages.

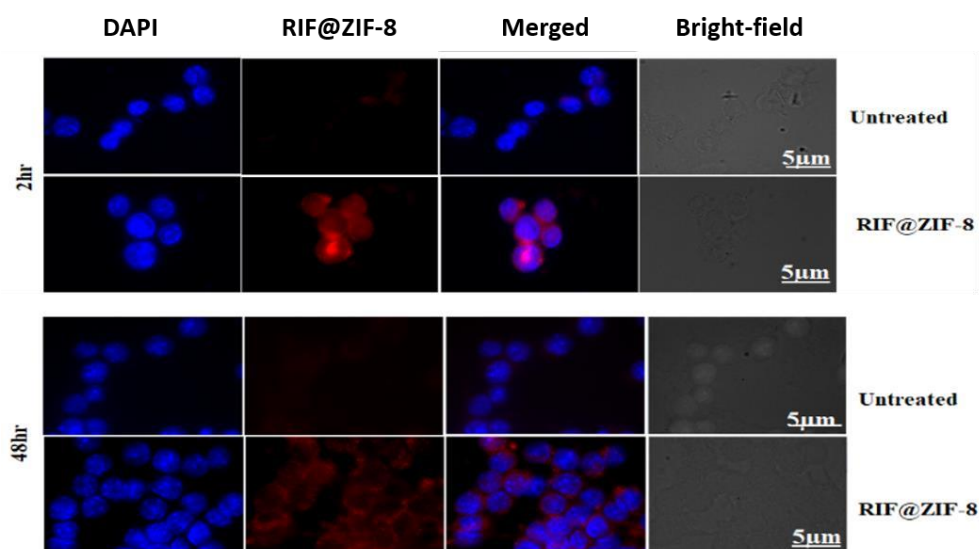


**Figure 5.13:** Cellular uptake of RIF@ZIF-8 by RAW 264.7 macrophages



## Chapter 5

### Conclusions and Future Directions

---

Conventional chemotherapy against tuberculosis is less efficacious due to its non-targeted drug delivery, longer treatment duration, and harmful side effects. The toxicity profile of any drug is checked to see whether it is detrimental to cells. Any medication should not be toxic to host cells as it causes side effects to human health. Rifampicin is an effective anti-TB first-line drug, but it can't eliminate drug-resistant strains and also has many side effects.

A novel approach is needed to improve TB therapy. Modifying conventional antibiotics and reengineering them using drug carriers to target drug delivery could be a safer and more efficient approach against TB. Studies on nanomaterials have shown antibacterial action, which especially offers insight into combating TB. Metal-organic frameworks (MOFs) are possible candidates for acting as drug carriers. Research studies of MOFs suggest that due to their structural features of large porosity, controlled drug release in a pH-dependent manner, large surface area, biocompatibility, and better release rate makes it a suitable candidate to act as an antibacterial agent.

Importantly, studies on ZIF-8 have shown pronounced antibacterial effects against Gram-positive & Gram-negative bacteria. Therefore, to address TB infections, encapsulating anti-TB drugs into MOFs and then checking the antibacterial activity would give more idea about the killing efficiency of encapsulated MOFs. We have successfully encapsulated rifampicin into ZIF-8 with high loading efficiency of 82 %. Synthesis and encapsulation were characterized with many techniques such as PXRD, FTIR, UV-VIS spectroscopy, SEM, TGA, and BET. Our studies conducted comparative studies on the cytotoxicity profile of encapsulated MOFs, drugs, and pure

MOFs. It was observed that RIF@ZIF-8 was not toxic till 40  $\mu\text{g/ml}$ . RIF@ZIF-8 was successfully taken up by macrophages within 2 hours.

Further studies on antibacterial properties and intracellular killing efficiency of RIF@ZIF-8 compared to alone rifampicin needs to be compared.

Developing nanomedicines for tuberculosis is a very efficient strategy to deliver old drugs and to make them more potent since the probability of a new TB drug coming to market soon is very low. In the future, MOFs can be created that contain all four first lines of drugs to smooth the treatment process. MOFs can also be created in such a manner that they can be an inhalable therapeutic to only target lungs as well as multiple surface modification can be performed for targeted therapy

## References

---

1. Cambier, C. J., Falkow, S., & Ramakrishnan, L. (2014). Host evasion and exploitation schemes of *Mycobacterium tuberculosis*. *Cell*, *159*(7), 1497-1509.
2. Chai, Q., Zhang, Y., & Liu, C. H. (2018). *Mycobacterium tuberculosis*: an adaptable pathogen associated with multiple human diseases. *Frontiers in cellular and infection microbiology*, *8*, 158.
3. Pai, M., Behr, M. A., Dowdy, D., Dheda, K., Divangahi, M., Boehme, C. C., Ginsberg, A., Swaminathan, S., Spigelman, M., Getahun, H., Menzies, D., & Raviglione, M. (2016). Tuberculosis. *Nature reviews. Disease primers*, *2*, 16076.
4. Chandra, P., Grigsby, S. J., & Philips, J. A. (2022). Immune evasion and provocation by *Mycobacterium tuberculosis*. *Nature Reviews Microbiology*, *20*(12), 750-766.
5. Sia, J. K., & Rengarajan, J. (2019). Immunology of *Mycobacterium tuberculosis* infections. *Microbiology spectrum*, *7*(4), 10-1128.
6. Jang, J. G., & Chung, J. H. (2020). Diagnosis and treatment of multidrug-resistant tuberculosis. *Yeungnam University journal of medicine*, *37*(4), 277-285.
7. World Health Organization. *Rapid Communication: Key Changes to Treatment of Multidrug- and Rifampicin-Resistant Tuberculosis*; WHO: Geneva, Switzerland, 2018; pp. 1-7.
8. Kumar, M., Virmani, T., Kumar, G., Deshmukh, R., Sharma, A., Duarte, S., Brandão, P., & Fonte, P. (2023). Nanocarriers in Tuberculosis Treatment: Challenges and Delivery Strategies. *Pharmaceuticals (Basel, Switzerland)*, *16*(10), 1360.
9. Bourguignon, T., Godinez-Leon, J. A., & Gref, R. (2023). Nanosized Drug Delivery Systems to Fight Tuberculosis. *Pharmaceutics*, *15*(2), 393.

10. Rothstein D. M. (2016). Rifamycins, Alone and in Combination. *Cold Spring Harbor perspectives in medicine*, 6(7), a027011.
11. Unissa, A. N., Subbian, S., Hanna, L. E., & Selvakumar, N. (2016). Overview on mechanisms of isoniazid action and resistance in Mycobacterium tuberculosis. *Infection, genetics and evolution : journal of molecular epidemiology and evolutionary genetics in infectious diseases*, 45, 474–492.
12. Njire, M., Tan, Y., Mugweru, J., Wang, C., Guo, J., Yew, W., Tan, S., & Zhang, T. (2016). Pyrazinamide resistance in Mycobacterium tuberculosis: Review and update. *Advances in medical sciences*, 61(1), 63–71.
13. Zhang, Y., Wade, M. M., Scorpio, A., Zhang, H., & Sun, Z. (2003). Mode of action of pyrazinamide: disruption of Mycobacterium tuberculosis membrane transport and energetics by pyrazinoic acid. *The Journal of antimicrobial chemotherapy*, 52(5), 790–795.
14. Takayama, K., Armstrong, E. L., Kunugi, K. A., & Kilburn, J. O. (1979). Inhibition by ethambutol of mycolic acid transfer into the cell wall of Mycobacterium smegmatis. *Antimicrobial agents and chemotherapy*, 16(2), 240–242.
15. Elnady, R. E., Amin, M. M., & Zakaria, M. Y. (2023). A review on lipid-based nanocarriers mimicking chylomicron and their potential in drug delivery and targeting infectious and cancerous diseases. *AAPS Open*, 9(1), 13.
16. Palomino, J. C., & Martin, A. (2014). Drug Resistance Mechanisms in Mycobacterium tuberculosis. *Antibiotics (Basel, Switzerland)*, 3(3), 317–340.
17. Nasiruddin, M., Neyaz, M. K., & Das, S. (2017). Nanotechnology-Based Approach in Tuberculosis Treatment. *Tuberculosis research and treatment*, 2017, 4920209.
18. Costa-Gouveia, J., Aínsa, J. A., Brodin, P., & Lucía, A. (2017). How can nanoparticles contribute to antituberculosis therapy?. *Drug discovery today*, 22(3), 600–607.

19. Virmani, T., Kumar, G., Virmani, R., Sharma, A., & Pathak, K. (2022). Nanocarrier-based approaches to combat chronic obstructive pulmonary disease. *Nanomedicine (London, England)*, *17*(24), 1833–1854.
20. Parveen, S., Sur, T., Sarkar, S., & Roy, R. (2023). Antagonist Impact of Selenium-Based Nanoparticles Against Mycobacterium tuberculosis. *Applied biochemistry and biotechnology*, *195*(6), 3606–3614.
21. Lin, W., Fan, S., Liao, K., Huang, Y., Cong, Y., Zhang, J., Jin, H., Zhao, Y., Ruan, Y., Lu, H., Yang, F., Wu, C., Zhao, D., Fu, Z., Zheng, B., Xu, J. F., & Pi, J. (2023). Engineering zinc oxide hybrid selenium nanoparticles for synergetic anti-tuberculosis treatment by combining Mycobacterium tuberculosis killings and host cell immunological inhibition. *Frontiers in cellular and infection microbiology*, *12*, 1074533.
22. Gaspar, M. M., Cruz, A., Penha, A. F., Reymão, J., Sousa, A. C., Eleutério, C. V., ... & Pedrosa, J. (2008). Rifabutin encapsulated in liposomes exhibits increased therapeutic activity in a model of disseminated tuberculosis. *International journal of antimicrobial agents*, *31*(1), 37-45.
23. Chowdhury, P., & Shankar, U. (2016). Formulation and evaluation of Rifampicin and Ofloxacin niosomes for Drugresistant TB on Logarithmic-phase cultures of Mycobacterium tuberculosis. *Int J Res Pharma Sci (IJRPS)*, *3*(4), 628-33.
24. Anjani, Q. K., Permana, A. D., Cárcamo-Martínez, Á., Domínguez-Robles, J., Tekko, I. A., Larrañeta, E., ... & Donnelly, R. F. (2021). Versatility of hydrogel-forming microneedles in in vitro transdermal delivery of tuberculosis drugs. *European Journal of Pharmaceutics and Biopharmaceutics*, *158*, 294-312.
25. Govindaraju, K., Vasantharaja, R., Suganya, K. U., Anbarasu, S., Revathy, K., Pugazhendhi, A., ... & Singaravelu, G. (2020). Unveiling the anticancer and antimycobacterial potentials of

- bioengineered gold nanoparticles. *Process Biochemistry*, 96, 213-219.
26. Zomorodbakhsh, S., Abbasian, Y., Naghinejad, M., & Sheikhpour, M. (2020). The effects study of isoniazid conjugated multi-wall carbon nanotubes nanofluid on Mycobacterium tuberculosis. *International journal of nanomedicine*, 5901-5909.
  27. Kumar, P. V., Asthana, A., Dutta, T., & Jain, N. K. (2006). Intracellular macrophage uptake of rifampicin loaded mannosylated dendrimers. *Journal of drug targeting*, 14(8), 546-556.
  28. Nair, A., Greeny, A., Nandan, A., Sah, R. K., Jose, A., Dyawanapelly, S., Junnuthula, V., K V, A., & Sadanandan, P. (2023). Advanced drug delivery and therapeutic strategies for tuberculosis treatment. *Journal of nanobiotechnology*, 21(1), 414.
  29. Yusuf, V. F., Malek, N. I., & Kailasa, S. K. (2022). Review on Metal-Organic Framework Classification, Synthetic Approaches, and Influencing Factors: Applications in Energy, Drug Delivery, and Wastewater Treatment. *ACS omega*, 7(49), 44507–44531.
  30. Lawson, H. D., Walton, S. P., & Chan, C. (2021). Metal-Organic Frameworks for Drug Delivery: A Design Perspective. *ACS applied materials & interfaces*, 13(6), 7004–7020.
  31. Gupta, C., Pant, P., & Rajput, H. (2022). Strategies to Synthesize Diverse Metal–Organic Frameworks (MOFs). In *Metal-Organic Frameworks (MOFs) as Catalysts* (pp. 69-97). Singapore: Springer Nature Singapore.
  32. Maleki, A., Shahbazi, M. A., Alinezhad, V., & Santos, H. A. (2020). The Progress and Prospect of Zeolitic Imidazolate Frameworks in Cancer Therapy, Antibacterial Activity, and Biomineralization. *Advanced healthcare materials*, 9(12), e2000248.
  33. Cai, W., Wang, J., Chu, C., Chen, W., Wu, C., & Liu, G. (2018). Metal-Organic Framework-Based Stimuli-Responsive Systems for Drug Delivery. *Advanced science (Weinheim, Baden-Wuerttemberg, Germany)*, 6(1), 1801526.

34. Qi, X., Shen, N., Al Othman, A., Mezentsev, A., Permyakova, A., Yu, Z., Lepoitevin, M., Serre, C., & Durymanov, M. (2023). Metal-Organic Framework-Based Nanomedicines for the Treatment of Intracellular Bacterial Infections. *Pharmaceutics*, *15*(5), 1521.
35. Zhang, X., , Liu, L., , Huang, L., , Zhang, W., , Wang, R., , Yue, T., , Sun, J., , Li, G., , & Wang, J., (2019). The highly efficient elimination of intracellular bacteria via a metal organic framework (MOF)-based three-in-one delivery system. *Nanoscale*, *11*(19), 9468–9477.
36. Simon, M. A., Anggraeni, E., Soetaredjo, F. E., Santoso, S. P., Irawaty, W., Thanh, T. C., Hartono, S. B., Yuliana, M., & Ismadji, S. (2019). Hydrothermal Synthesize of HF-Free MIL-100(Fe) for Isoniazid-Drug Delivery. *Scientific reports*, *9*(1), 16907.
37. Li, Y., Zheng, Y., Lai, X., Chu, Y., & Chen, Y. (2018). Biocompatible surface modification of nano-scale zeolitic imidazolate frameworks for enhanced drug delivery. *RSC advances*, *8*(42), 23623-23628.
38. Sun, C. Y., Qin, C., Wang, X. L., Yang, G. S., Shao, K. Z., Lan, Y. Q., Su, Z. M., Huang, P., Wang, C. G., & Wang, E. B. (2012). Zeolitic Imidazolate framework-8 as efficient pH-sensitive drug delivery vehicle. *Dalton transactions (Cambridge, England : 2003)*, *41*(23), 6906–6909.
39. Nabipour, H., Sadr, M. H., & Bardajee, G. R. (2017). Synthesis and characterization of nanoscale zeolitic imidazolate frameworks with ciprofloxacin and their applications as antimicrobial agents. *New Journal of Chemistry*, *41*(15), 7364-7370.
40. Soltani, B., Nabipour, H., & Nasab, N. A. (2018). Efficient storage of gentamicin in nanoscale zeolitic imidazolate framework-8 nanocarrier for pH-responsive drug release. *Journal of Inorganic and Organometallic Polymers and Materials*, *28*, 1090-1097.
41. Soomro, N. A., Wu, Q., Amur, S. A., Liang, H., Rahman, A. U., Yuan, Q., & Wei, Y. (2019). Natural drug physcion encapsulated zeolitic imidazolate framework, and their application as

- antimicrobial agent. *Colloids and Surfaces B: Biointerfaces*, 182, 110364.
42. Sava Gallis, D. F., Butler, K. S., Agola, J. O., Pearce, C. J., & McBride, A. A. (2019). Antibacterial countermeasures via metal–organic framework-supported sustained therapeutic release. *ACS applied materials & interfaces*, 11(8), 7782-7791.
43. Chowdhuri, A. R., Das, B., Kumar, A., Tripathy, S., Roy, S., & Sahu, S. K. (2017). One-pot synthesis of multifunctional nanoscale metal-organic frameworks as an effective antibacterial agent against multidrug-resistant *Staphylococcus aureus*. *Nanotechnology*, 28(9), 095102.
44. Kumar, P., Behera, A., Tiwari, P., Karthik, S., Biswas, M., Sonawane, A., & Mobin, S. M. (2023). Exploring the antimicrobial potential of isoniazid loaded Cu-based metal-organic frameworks as a novel strategy for effective killing of *Mycobacterium tuberculosis*. *Journal of materials chemistry. B*, 11(45), 10929–10940.
45. Pan, Y., Liu, Y., Zeng, G., Zhao, L., & Lai, Z. (2011). Rapid synthesis of zeolitic imidazolate framework-8 (ZIF-8) nanocrystals in an aqueous system. *Chemical communications (Cambridge, England)*, 47(7), 2071–2073.
46. El-Bindary, A. A., Toson, E. A., Shoueir, K. R., Aljohani, H. A., & Abo-Ser, M. M. (2020). Metal–organic frameworks as efficient materials for drug delivery: Synthesis, characterization, antioxidant, anticancer, antibacterial and molecular docking investigation. *Applied Organometallic Chemistry*, 34(11), e5905.
47. Tran, V. A., & Lee, S. W. (2021). pH-triggered degradation and release of doxorubicin from zeolitic imidazolate framework-8 (ZIF8) decorated with polyacrylic acid. *RSC advances*, 11(16), 9222–9234.
48. Zhang, Y., Jia, Y., & Hou, L. (2018). Synthesis of zeolitic imidazolate framework-8 on polyester fiber for PM<sub>2.5</sub> removal. *RSC advances*, 8(55), 31471–31477.

49. Howarth, A. J., Peters, A. W., Vermeulen, N. A., Wang, T. C., Hupp, J. T., & Farha, O. K. (2017). Best practices for the synthesis, activation, and characterization of metal–organic frameworks. *Chemistry of Materials*, 29(1), 26-39.
50. Mondloch, J. E., Karagiari, O., Farha, O. K., & Hupp, J. T. (2013). Activation of metal–organic framework materials. *CrystEngComm*, 15(45), 9258-9264.
51. Siva, V., Murugan, A., Shameem, A., Thangarasu, S., & Bahadur, S. A. (2022). A simple synthesis method of zeolitic imidazolate framework-8 (ZIF-8) nanocrystals as superior electrode material for energy storage systems. *Journal of Inorganic and Organometallic Polymers and Materials*, 32(12), 4707-4714.